

LIB

AGARDograph 119

AGARDograph 119

AGARD

ADVISORY GROUP FOR AEROSPACE RESEARCH & DEVELOPMENT

64 RUE DE VARENNE PARIS 7^E FRANCE

Thermo-Molecular Pressure Effects in Tubes and at Orifices

by Max Kinslow and George D. Arney, Jr

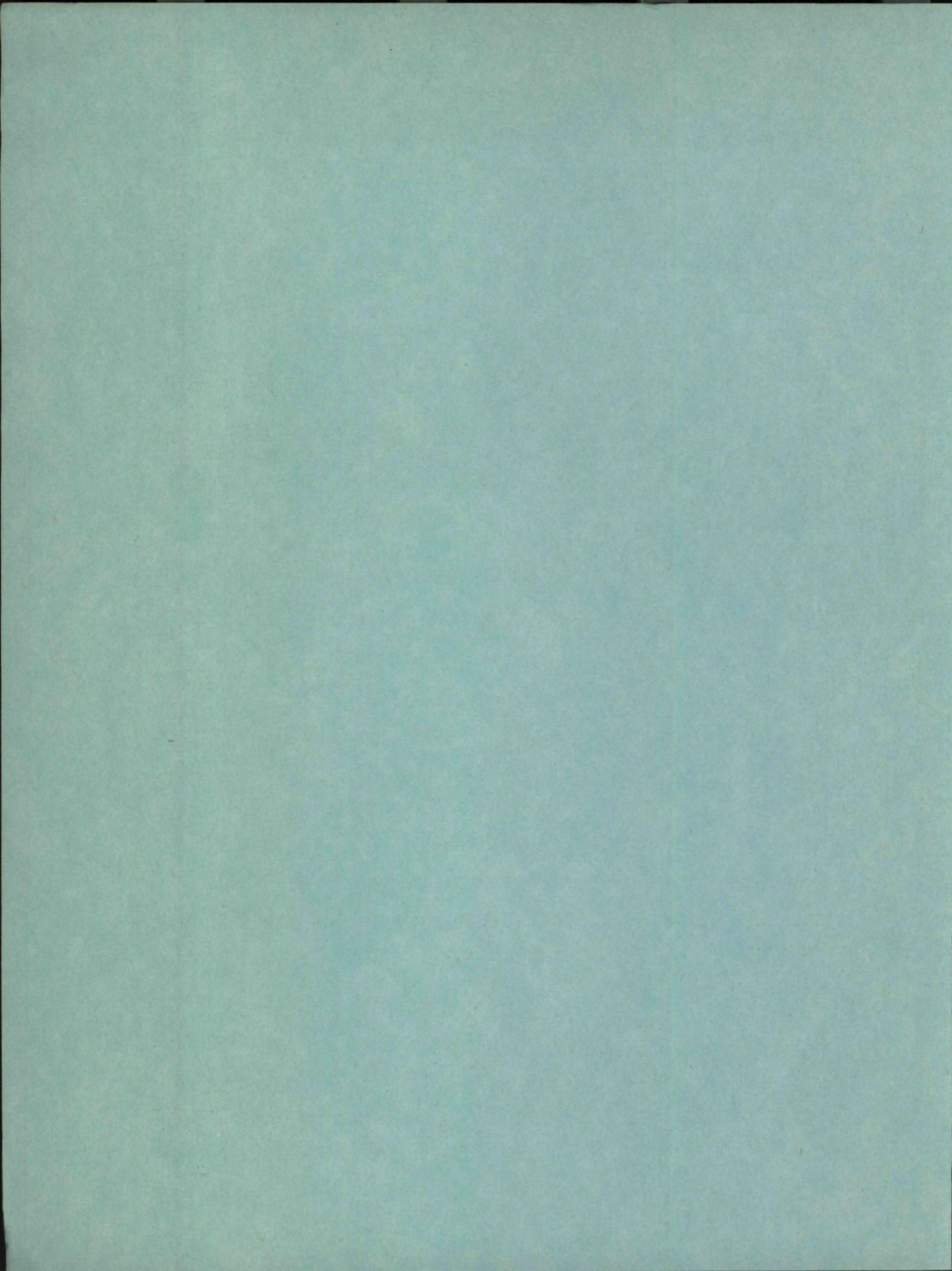


AUGUST 1967

ROYAL AIRCRAFT
ESTABLISHMENT
13 DEC 1967
LIBRARY

NORTH ATLANTIC TREATY ORGANIZATION





NORTH ATLANTIC TREATY ORGANIZATION
ADVISORY GROUP FOR AEROSPACE RESEARCH AND DEVELOPMENT
(ORGANISATION DU TRAITE DE L'ATLANTIQUE NORD)

THERMO-MOLECULAR PRESSURE EFFECTS
IN TUBES AND AT ORIFICES

by

Max Kinslow and George D. Arney, Jr

ARO, Inc.
Arnold Air Force Station, Tennessee, USA

August 1967

SUMMARY

An investigation of the errors arising from thermal nonequilibrium in systems measuring gas pressures is presented. The errors are attributed to a phenomenon referred to as thermo-molecular pressure. This effect is investigated both theoretically and experimentally at sensing orifices and in tubes. A thorough review of the literature is given and a theory is developed for the error introduced in the limiting case of a very small sensing orifice with heat flux to the orifice surface. The theory takes into account the effect of arbitrary thermal accommodation coefficient at the orifice surface. Experimental data are presented separately for thermo-molecular pressures in tubes and at orifices. In addition, results of heat-transfer measurements in the transitional flow regime between flat plates are presented as a basis for correlating the orifice data. Finally, methods are given, with examples, for the correction of thermo-molecular effects both at orifices and in circular tubes.

RESUME

Ce rapport traite des erreurs dûs au non-équilibre thermique dans des dispositifs de mesure des pressions de gaz. Les erreurs sont attribuées à un phénomène dit la pression thermomoléculaire. Cet effet est étudié en théorie et par l'expérience sur des orifices de sondage et en tubes. La littérature est passée en revue assez profondément et une théorie est proposée pour l'erreur introduite dans le cas limite d'un très petit orifice de sondage avec un flux de chaleur vers la surface d'orifice. La théorie tient compte de l'effet d'un coefficient de correction thermique arbitraire sur la surface d'orifice. Des données expérimentales sont présentées pour des pressions thermomoléculaires en tubes d'une part, et sur les orifices d'autre part. De plus, les résultats des mesures sont présentés pour le transfert de chaleur en régime d'écoulement de transition entre plaques planes formant une base de corrélation des données d'orifices. Enfin, on donne des méthodes et des exemples pour la correction des effets thermomoléculaires sur des orifices aussi bien qu'en tubes circulaires.

532.522:532.575.6

CONTENTS

	Page
SUMMARY	ii
RESUME	ii
LIST OF FIGURES	iv
NOTATION	vi
1. INTRODUCTION	1
2. REVIEW OF PREVIOUS INVESTIGATIONS	3
2.1 Effect in Tubes and Porous Materials	3
2.2 Effect at Orifices	4
3. THEORETICAL ANALYSIS	5
3.1 Existing Theories of Thermo-Molecular Pressure in Tubes	5
3.2 Analysis of the Effect at Orifices with Heat Flux	6
4. EXPERIMENTAL APPARATUS AND PROCEDURE	11
5. DISCUSSION OF RESULTS	13
5.1 Thermo-Molecular Pressure in Tubes	13
5.2 Heat Transfer	16
5.3 Thermo-Molecular Pressure at Orifices	17
6. APPLICATION OF RESULTS	19
6.1 Tube Effect	19
6.2 Orifice Effect	21
ACKNOWLEDGMENT	23
REFERENCES	24
FIGURES	26
DISTRIBUTION	

LIST OF FIGURES

		Page
Fig. 1	Plot of Equation (27)	26
Fig. 2	Plot of modified Equation (27)	27
Fig. 3	Sketch of apparatus	28
Fig. 4	Photograph of apparatus	29
Fig. 5	Tube and orifice schedule	30
Fig. 6	Slip flow results for tubes using hydrogen	31
Fig. 7	Slip flow results for tubes using helium	32
Fig. 8	Slip flow results for tubes using nitrogen	33
Fig. 9	Slip flow results for tubes using argon	34
Fig. 10	Mean free path for gases tested	35
Fig. 11	Transitional results for tubes using hydrogen	36
Fig. 12	Transitional results for tubes using helium	37
Fig. 13	Transitional results for tubes using nitrogen	38
Fig. 14	Transitional results for tubes using argon	39
Fig. 15	Determination of α from measured \dot{q} for hydrogen	40
Fig. 16	Determination of α from measured \dot{q} for helium	41
Fig. 17	Determination of α from measured \dot{q} for nitrogen	42
Fig. 18	Determination of α from measured \dot{q} for argon	43
Fig. 19	Summary of heat-transfer results for all gases tested	44
Fig. 20	Experimental results for circular orifices using hydrogen	45

	Page
Fig. 21	Experimental results for circular orifices using helium 46
Fig. 22	Experimental results for circular orifices using nitrogen 47
Fig. 23	Experimental results for circular orifices using argon 48
Fig. 24	Experimental results for annular orifices for all gases tested 49
Fig. 25	Combined theoretical and experimental results for orifices 50-57

NOTATION

a		orifice length
B	=	$(8/15)h/\lambda_w^+$
d		diameter of orifice
f		velocity distribution function
g		slot width
h		plate spacing
J		defined by Equation (30)
Kn		Knudsen number, ratio of mean free path to characteristic length
Kn_c	=	$\lambda(T_c, p_c)/r$
Kn_h	=	$\lambda(T_h, p_h)/r$
$Kn_{w, i, d}$	=	$\lambda(T_w, p_i)/d$
$Kn_{w, i, g}$	=	$\lambda(T_w, p_i)/g$
$Kn_{w, i, h}$	=	$\lambda(T_w/p_i)/h$
$Kn_{w, w, h}$	=	$\lambda(T_w/p_w)/h$
k		thermal conductivity
L	=	$\sqrt{(T_i^-/T_w^+)}$
l		length of tube
M		molecular weight
m		mass of a molecule
N		molecular flux, molecules/unit area/unit time
N_{out}		flux of molecules leaving the sensing cavity
n		number density of molecules
p		pressure
\bar{p}	=	$[p_i - p_i]_{d \rightarrow 0} / [p_w - p_i]_{d \rightarrow 0}$

p_i	pressure indicated by sensing cavity
$p_i)_{d \rightarrow 0}$	pressure indicated by an infinitely small orifice
\dot{q}	energy flux, energy/unit area/unit time
\dot{q}_c	continuum heat flux given by Equation (39)
\dot{q}_{int}	internal energy flux
\dot{q}_t	theoretical energy flux defined in Equation (33)
$\dot{q}_t)_c$	theoretical continuum heat flux given by Equation (41)
\dot{q}_{tr}	translational energy flux
r	radius of tube
s	exponent in Equation (36)
T	absolute temperature
X	defined by Equation (35)
x	axial distance along a tube
y	coordinate normal to plates
Z	defined by Equation (36)
α	thermal accommodation coefficient
γ	ratio of specific heats
ζ	slip distance at a wall
κ	$= \dot{q}(\gamma - 1) / [p_i \sqrt{(RT_w)} (\gamma + 1)]$
$\lambda(T, p)$	mean free path, given by Equation (37)
μ	viscosity or pressure in microns of Hg
$\xi_{x, y, z}$	molecular velocity components
ρ	mass density
ω	probability that a molecule entering a tube will exit at the other end

Subscripts

- 1 conditions at source plate for orifice effect and at one end of tube for tube effect
- 2 conditions at other end of tube for tube effect
- c condition at cold end of tube
- h condition at hot end of tube
- w conditions at wall

Superscripts

- + molecules with $\xi_y > 0$
- molecules with $\xi_y < 0$

THERMO-MOLECULAR PRESSURE EFFECTS IN TUBES AND AT ORIFICES

Max Kinslow and George D. Arney, Jr

1. INTRODUCTION

Where there is thermal nonequilibrium in a gas, particularly under rarefied condition, certain phenomena occur which Knudsen¹, in 1910, termed thermo-molecular. In particular, thermo-molecular pressure is a term meant to imply the phenomenon wherein a pressure difference or gradient is produced by a temperature difference or gradient. Under low-density conditions with accompanying thermal gradients, the determination of pressures by usual methods involving orifices and connecting tubing may be liable to appreciable error because of this phenomenon.

As the title implies, thermo-molecular pressures at orifices and in tubes are to be treated separately and independently throughout this investigation. While it is conceivable that a condition might exist where such a separation would be difficult, the independent treatment can usually be justified, especially if the problem is considered before designing a pressure measuring system.

In this paper the term equilibrium will be synonymous with complete thermodynamic equilibrium, which requires thermal, mechanical, and chemical equilibrium; i. e., there is no gradient of any property* such as temperature or pressure. In the past, in papers dealing with the present subject, many authors have used the term 'equilibrium' to mean steady state, or invariant with time. These uses of the term equilibrium may cause confusion, but luckily, in most situations involving higher densities with energy flux or velocity gradient, the use of equilibrium equations is usually justified. However, at sufficiently low pressure, the concept of a gas temperature may lose its meaning. At a given point in space, molecules traveling in different directions may have, loosely speaking, different temperatures, depending upon where they originated, assuming of course that they come from a point in the gas close to equilibrium or from a surface so that a temperature can be defined. Under consideration is the phenomenon whereby mechanical nonequilibrium (pressure gradient) is produced by thermal nonequilibrium (temperature gradient). Normally, under conditions of higher density, these two forms of nonequilibrium are considered completely independent. This probably accounts, in part, for the fact that thermo-molecular pressures are a relatively obscure subject, especially to those new to the field of rarefied gases.

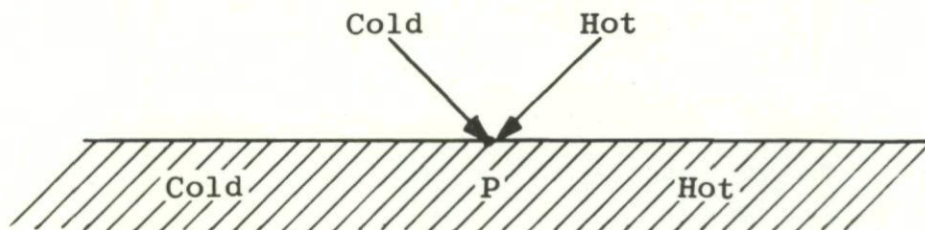
While many types of pressure measurements may be affected, some of the more interesting manifestations of the orifice effect have been in connection with impact-pressure probes (cf. Bailey and Boylan² and Bailey³). In this case, the subject should not be

* Neglecting external forces, for example, gravitational forces which produce a pressure gradient.

confused with the more widely known variation of impact pressure with probe Reynolds number when the orifice size is not a matter of particular concern (see Potter and Bailey⁴). It is also evident that various other types of aerodynamic pressure measurements may be seriously affected, e.g., hypersonic, viscous, pressure interaction data. Also affected may be the measurement of pressure in any low pressure environment where temperature extremes exist. For example, high temperature components heated for the purpose of outgassing, cold traps, or cryogenic components are sources of possible errors.

Returning now to the basic phenomena of thermo-molecular pressures, two other terms will be discussed briefly to remove possible confusion. In the past 'thermal creep' and 'thermal transpiration' have been applied to specific thermo-molecular effects. Both these terms carry with them the connotation of a flow. Thermal creep is applied to the phenomena of the flow of a gas over a surface with a nonuniform temperature. There is a tendency for the gas adjacent to the surface to flow from cooler regions to hotter regions.

A qualitative explanation of thermal creep can be based on the accompanying sketch.



A temperature gradient exists along the wall which induces a temperature gradient in the gas not necessarily equal to the one in the wall, although the direction will be the same. Assume that the mass of gas is stationary, then at any point P equal numbers of molecules pass a plane perpendicular to the surface at P from hot to cold as from cold to hot. The gas molecules striking near point P coming from the region of the hot gas have a higher velocity and therefore greater momentum than those coming from the colder regions of the gas. For a nonspecular reflection, there results a net momentum transfer tangential to the surface. From Newton's third law there must be an equal and opposite force acting on the gas. If conditions are such as to prevent a continuing flow of gas, then a pressure gradient will be established so that the net force on the gas is zero. Otherwise the gas will flow or creep along the surface such that the net force to the wall is zero. For a more complete treatment of thermal creep the reader is referred to the text of Kennard⁵.

The term 'thermal transpiration' originally was used to describe the phenomenon of the effusion of gases through a porous material when there is a temperature difference in the gas on each side or a temperature gradient in the material. As is the occurrence with thermal creep, if a steady flow is not permitted, then a pressure difference across the porous membrane will be established. At low pressures the quantity p/\sqrt{T} will be the same on each side (cf. Reference 5). Thermal transpiration can be demonstrated at fairly high pressures across a porous material because the pores can be extremely small; however, it is difficult to obtain quantitative data because there is usually no single relevant characteristic length to associate with the material. Thermal transpiration as just described will not be considered further.

2. REVIEW OF PREVIOUS INVESTIGATIONS

2.1 Effect in Tubes and Porous Materials

Neumann⁶, in 1872, made the first recorded observation of thermo-molecular pressures. The following year Feddersen⁷ reported the results of experiments using powdery materials, spongy platinum, and spongy palladium and confirmed that there was a variation of pressure with temperature across the material. Neumann and Feddersen both termed this phenomenon thermodiffusion, thinking it to be due to the difference in adsorption or absorption of gases at different temperatures. However, it was later shown by Reynolds⁸ that from a kinetic theory viewpoint, in the absence of flow of the gas through the plug, the quantity p/\sqrt{T} should be expected to be constant across the material, independent of adsorption or absorption. Reynolds proved experimentally, using plugs of plaster of Paris and meerschaum, that at low pressures the pressures on the two sides of the plug are indeed related by $p_1/p_2 = \sqrt{T_1/T_2}$. Reynolds referred to the phenomenon as thermal transpiration.

From a similar kinetic theory viewpoint, it was shown by Maxwell⁹ in 1879 that, if a temperature gradient exists along a tube containing a mass of gas such that the mean free path is very large compared to the tube radius, and if conditions are such that no net flow of the gas in the tube is permitted, then throughout the tube the quantity p/\sqrt{T} is to be expected to remain constant, or in differential form $(dT/dp)(p/2T) = 1$. This relation has often been referred to as the free molecular limit since the analysis requires that $\lambda \gg r$. Of course at the other extreme, where $\lambda \ll r$, there is the continuum limit where the pressure is constant throughout.

Maxwell also attacked the more difficult problem of analyzing the situation in a tube containing a mass of gas such that there existed what is now known as the slip flow regime. By equating the thermal creep along the surface of the tube to the reverse Poiseuille flow in the central portion, there resulted, using present nomenclature, the theoretical relation

$$\frac{dp}{dT} = \left[\frac{6\mu^2}{\rho T r^2} \right] \left[\frac{1}{1 + 4\zeta/r} \right] \quad (1)$$

Some thirty years later, in 1910, the first qualitative data on gases in tubes were obtained by Knudsen¹, who proposed the terms thermo-molecular flow and thermo-molecular pressure to replace previously used terms. Knudsen's extensive study, both theoretical and experimental, is perhaps the most important contribution to the understanding of thermo-molecular phenomena in tubes. Like Maxwell, Knudsen obtained an expression for the thermo-molecular pressure effect for both the free molecular limit and the slip flow regime¹⁰. Knudsen's result was the same for the free molecular limit and of the same form as Maxwell's for the slip flow regime (Equation (1)) with the viscosity μ replaced by the then generally accepted expression. In addition, Knudsen obtained theoretically, for the near free molecular regime, the relation¹

$$\frac{dp}{dT} = \left[\frac{p}{2T} \right] \left[\frac{1}{1 + 2r/\lambda} \right], \quad (\lambda \gg r) \quad (2)$$

His extensive investigation culminated in 1927 with the publication¹¹, for all regimes from the free molecular to the continuum limit, of the relation

$$\frac{dp}{dT} = \frac{p/2T}{\left[1 + 2.46 \frac{r}{\lambda} \frac{(1 + 3.15r/\lambda)}{(1 + 24.5r/\lambda)} \right]^2} \quad (3)$$

This relation was obtained from work with hydrogen using glass tubes.

Tompkins and Wheeler¹² also obtained a small amount of data for hydrogen in glass tubes. Unfortunately, data were insufficient to significantly add to what Knudsen and others had done formerly.

In much more recent years Howard¹³ was perhaps the first to obtain thermo-molecular pressure data in metal tubing. Howard's results, in general, confirm those of Knudsen. However, at higher temperature there is some disagreement between Knudsen's semi-empirical equation and Howard's data. Knudsen himself had observed the same discrepancy at high temperature and had attributed it to his calculation of mean free path.

Arney and Bailey¹⁴ have obtained a wealth of data for metal tubes and various gases at several temperature ratios. They too disagree with Knudsen (Equation (3)) at higher temperatures.

While all the aforementioned investigators obtained results that were in substantial agreement with each other, there were deficiencies common to all of the experimental procedures. All investigators measured pressure with gages at or near room temperature and at locations remote from the point in the tubes where direct measurement was desirable. The very phenomena being investigated made invalid certain of the measurements. The procedure was to measure the difference in the thermo-molecular pressure for a large diameter tube and a small diameter tube and to determine the thermo-molecular pressure across each by a 'boot-strap' technique. The success of this technique depends upon the ratio of tube diameters that can be used and the accuracy of the measurements. Any small systematic error tends to be magnified in the transition regime. Also, all previous experiments were conducted using relatively long tubes. While it is true that the free molecule limit is independent of tube length, it is conceivable that length would be a factor in the transitional regime.

2.2 Effect at Orifices

Only recently, in a paper by one of the present authors and colleagues¹⁵, attention was called to the fact that large thermo-molecular pressure effects can exist at pressure-sensing orifices where there is heat flux to the orifice surface. This paper was based on the assumption of a two-sided Maxwellian distribution function, which permitted a theoretical analysis for the limiting case of a very small orifice, and on a series of experiments where a heated plate was placed near the cooler orifice surface to create the heat flux situation. While admitting to possible limitations in their experiment because of Knudsen manometer effects and uncertainties in heat-transfer rates, the authors presented results throughout the transitional regime which demonstrate that thermo-molecular pressures at orifices can be very significant.

3. THEORETICAL ANALYSIS

3.1 Existing Theories of Thermo-Molecular Pressure in Tubes

Returning to Maxwell's slip flow result (Equation (1)) and defining mean free path as

$$\lambda(T, p) = \frac{16}{5\sqrt{2\pi}} \left(\frac{\mu(T)}{p} \right) \sqrt{RT} ,$$

one obtains

$$\frac{dT}{dp} \frac{p}{2T} = \frac{256}{600\pi} \left(\frac{r}{\lambda} \right)^2 \cdot \left(1 + 4 \frac{\zeta}{\lambda} \frac{\lambda}{r} \right) \quad (4)$$

for $\lambda/r \ll 1$. The grouping on the left side of this equation was chosen because it approaches unity for the free molecule limit. Since $\lambda/r \ll 1$, the square root of Equation (4) can be approximated by

$$\begin{aligned} \sqrt{\left(\frac{dT}{dp} \frac{p}{2T} \right)} &\simeq 0.3686 \frac{r}{\lambda} \left(1 + 2 \frac{\zeta}{\lambda} \frac{\lambda}{r} \right) \\ &\simeq 0.3686 \frac{r}{\lambda} + 0.7372 \frac{\zeta}{\lambda} . \end{aligned} \quad (5)$$

Thus, from Maxwell's result for the slip flow regime, $\sqrt{\{(dT/dp)(p/2T)\}}$ should be a linear function of r/λ . Notice that if $\lambda/\zeta = 0.7372$, Equation (5) would give the correct free molecule limit as $r/\lambda \rightarrow 0$, i.e., $\sqrt{\{(dT/dp)(p/2T)\}} = 1$. However, this fact alone would not justify the use of Equation (5) outside the range of validity of the assumption used in its derivation. It will be shown later that the form of Equation (5) fits the experimental results over a far greater range than would be expected in view of the assumption made.

Knudsen's near free molecule result (Equation (2)) can be written as

$$\frac{dT}{dp} \frac{p}{2T} = 1 + 2 \frac{r}{\lambda} . \quad (6)$$

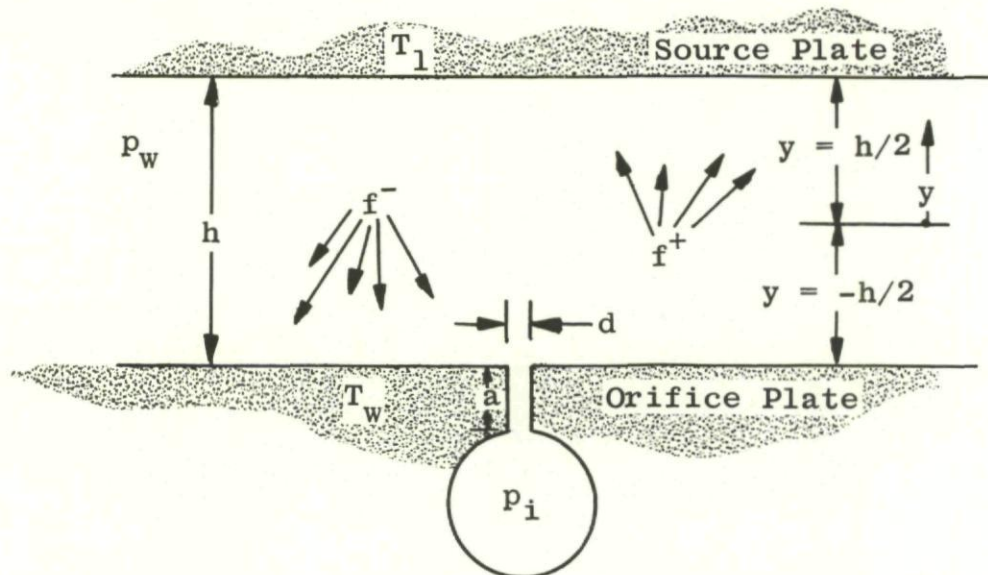
In order to compare this result with the slip flow result, take the square root of both sides of Equation (6) and approximate the square root of the right-hand side on the basis that $r/\lambda \ll 1$. This gives

$$\sqrt{\left(\frac{dT}{dp} \frac{p}{2T} \right)} = 1 + \frac{r}{\lambda} . \quad (7)$$

Thus the simplified theoretical equations for the thermo-molecular pressure effects in tubes can be reduced to linear equations for both the slip flow regime and the near free molecule regime. It is therefore reasonable to expect that the quantity $\sqrt{\{(dT/dp)(p/2T)\}}$ may form a basis for correlation of experimental data throughout all regimes.

3.2 Analysis of the Effect at Orifices with Heat Flux

Consider a small circular orifice* of diameter d in a surface or wall at a temperature T_w connected to a pressure-sensing cavity. The indicated pressure in this cavity is p_i . Let the surface be subject to a flux of energy from an adjacent gas. It is assumed that the thermo-molecular effects due to this heat transfer are independent of the mechanism causing the energy flux. Thus, we may imagine that the transfer of energy is caused by a plate at a temperature T_1 , as shown in the accompanying sketch.



The pressure in the gas is independent of the normal coordinate y (see Liu and Lees¹⁶) and is equal to the normal force per unit area on the wall, p_w . The indicated pressure p_i will equal p_w only if the gas near the wall is in complete equilibrium, e.g., no flux of energy or transverse momentum. The only type of nonequilibrium to be analyzed here is that arising from heat flux, although other modes can exist, for example, if there is a flow tangential to the surface. In any case the force per unit area on a surface is determined by the exchange of normal momentum between the gas and the walls. In the theoretical analysis that follows it is assumed that the orifice diameter is small compared to the mean free path in the gas, i.e., $Kn_d \gg 1$. The theoretical results are independent of the pressure between the plates and also the plate spacing; thus they apply for

$$0 \leq Kn_h \leq \infty.$$

If the Maxwell-Boltzmann velocity distribution function $f(x, y, z, \xi_x, \xi_y, \xi_z, t)$ were known, the flux of molecules, the energy, and the momentum at the surface or at any other point could be determined. The total number of molecules striking the surface of the plate or entering a small orifice in that plate is, per unit time and unit area,

$$N = \int_{-\infty}^{\infty} \int_{-\infty}^0 \int_{-\infty}^{\infty} f_{y=-h/2} \xi_y d\xi_x d\xi_y d\xi_z. \quad (8)$$

* The theoretical results that will follow are independent of the shape of the orifice, as long as a relevant dimension of the orifice is small. A circular orifice is chosen because this is usually the situation, and the diameter is convenient to carry through the analysis as the characteristic dimension.

Changing the limits on ξ_y to 0 to $+\infty$ gives the number of molecules emanating from the surface per unit time per unit area. The total normal momentum imparted to the wall w per unit area per unit time is equal to the pressure p_w . Then

$$p_w = m \int_{-\infty}^{\infty} \int_{-\infty}^{\infty} \int_{-\infty}^{\infty} f_{y=-h/2} \xi_y^2 d\xi_x d\xi_y d\xi_z . \quad (9)$$

Likewise, the energy flux to the surface, due to the translation energy of the molecules, is

$$\dot{q}_t = \frac{m}{2} \int_{-\infty}^{\infty} \int_{-\infty}^{\infty} \int_{-\infty}^{\infty} f_{y=-h/2} \xi_y [\xi_x^2 + \xi_y^2 + \xi_z^2] d\xi_x d\xi_y d\xi_z . \quad (10)$$

However, an exact, closed-form solution for f is known only for the case wherein there is no variation of f with position or time. This solution is the well-known Maxwellian velocity distribution which, for no mass motion, is

$$f = \frac{n}{(2\pi RT)^{3/2}} \exp\left(-\frac{\xi_x^2 + \xi_y^2 + \xi_z^2}{2RT}\right) . \quad (11)$$

Lees¹⁷ has proposed an approximation to f when thermal and velocity gradients are present that consists of using two half-range Maxwellian distributions chosen so that lower moments, such as Equations (8), (9), and (10), are equal to those of the actual distribution functions. This two-sided distribution was applied to the problem of plane compressible Couette flow with temperature gradients by Liu and Lees¹⁶.

Liu and Lees assumed that the molecules reflected from both plates were completely accommodated to the plate temperature. In order to be more general in the present analysis, an arbitrary accommodation coefficient is used. However, the results of Liu and Lees are still valid if the boundary conditions are slightly modified. Let molecules moving away from the orifice plate ($\xi_y > 0$) be identified by a superscript $+$ and molecules moving away from the source plate ($\xi_y < 0$) by a superscript $-$. The boundary conditions become $T^+ = T_w^+$ at $y = -h/2$ and $T^- = T_1^-$ at $y = h/2$. The thermal accommodation coefficient is defined as

$$\alpha_w = \frac{T_w^- - T_w^+}{T_w^- - T_w} \quad (12)$$

at the plate containing the orifice and

$$\alpha_1 = \frac{T_1^+ - T_1^-}{T_1^+ - T_1} \quad (13)$$

at the source plate.

Then, from Liu and Lees, using present nomenclature,

$$f = f^+ = \frac{n^+(y)}{[2\pi RT^+(y)]^{3/2}} \exp\left(-\frac{\xi_x^2 + \xi_y^2 + \xi_z^2}{2RT^+(y)}\right) \quad (14a)$$

for $\xi_y > 0$, and

$$f = f^- = \frac{n^-(y)}{[2\pi RT^-(y)]^{3/2}} \exp\left(-\frac{\xi_x^2 + \xi_y^2 + \xi_z^2}{2RT^-(y)}\right) \quad (14b)$$

for $\xi_y < 0$. The four functions $n^+(y)$, $n^-(y)$, $T^+(y)$, and $T^-(y)$ are to be determined from moment equations and the boundary conditions.

However, before specifying an intermolecular force law and solving for these four unknowns, it will be enlightening to continue as far as possible to determine what general results are independent of the interaction between molecules.

Using f as given by Equation (14) in Equations (8), (9), and (10) yields, from Equation (8),

$$N_w^- = n_w^- \sqrt{\left(\frac{RT_w^-}{2\pi}\right)} \quad (15)$$

or, changing the limits on ξ_y in Equation (8),

$$N_w^+ = n_w^+ \sqrt{\left(\frac{RT_w^+}{2\pi}\right)}. \quad (16)$$

From Equation (9),

$$p_w = \frac{1}{2} m R n_w^- T_w^- + \frac{1}{2} m R n_w^+ T_w^+ \quad (17)$$

and Equation (10) yields

$$\dot{q}_{tr} = \frac{2mn_w^+}{\sqrt{2\pi}} (RT_w^+)^{3/2} - \frac{2mn_w^-}{\sqrt{2\pi}} (RT_w^-)^{3/2}. \quad (18)$$

Using the principle of the equipartition of energy, each molecule carries, on the average, an internal energy of $[(5 - 3\gamma)/(\gamma - 1)][mRT/2]$. Assuming that the internal temperature of a molecule is equal to the corresponding translational temperature, the flux of internal energy becomes

$$\dot{q}_{int} = N_w^+ \left(\frac{5 - 3\gamma}{\gamma - 1}\right) \frac{mRT_w^+}{2} - N_w^- \left(\frac{5 - 3\gamma}{\gamma - 1}\right) \frac{mRT_w^-}{2}. \quad (19)$$

The total theoretical energy flux, obtained by adding Equations (18) and (19) and substituting Equations (15) and (16), becomes

$$\dot{q} = \frac{n_w^+ m (RT_w^+)^{3/2}}{2\sqrt{2\pi}} \left(\frac{\gamma + 1}{\gamma - 1}\right) - \frac{n_w^- m (RT_w^-)^{3/2}}{2\sqrt{2\pi}} \left(\frac{\gamma + 1}{\gamma - 1}\right). \quad (20)$$

Turning attention to the orifice cavity, let us see what results are forthcoming for the special case of small orifice diameter ($d \ll \lambda$). Henceforth, the pressure indicated by a cavity connected to a small orifice will be identified by $p_{i,d \rightarrow 0}$ to differentiate between the pressure p_i measured by means of an orifice of finite size. The number of molecules leaving the cavity per unit time per unit area is given by the equation for effusive flow because $d \ll \lambda$. For a finite length of orifice, a , not all the molecules leaving the cavity will leave the orifice at the surface of the plate since some will re-enter the orifice (e.g., those molecules striking the wall of the orifice and re-emitted toward the sensing cavity). It can be shown that the average probability, ω , of a molecule finding its way through the orifice tube after entering the orifice is a function only of the ratio a/d and the mass velocity normal to the plate surface. (See de Leeuw and Rothe¹⁸ or Clausing¹⁹). Because the normal mass velocity is zero at both the plate surface and the sensing cavity, the probability of transmission of a molecule entering the orifice from either end is the same. From almost any kinetic theory text (e.g., Present²⁰), the number flux of molecules for effusive flow is

$$N_{\text{out}} = \frac{p_{i,d \rightarrow 0}}{m\sqrt{2\pi RT_w}} \quad (21)$$

From the preceding discussion the number flux of molecules leaving the orifice at the surface of the plate is ωN_{out} . The number flux of molecules entering the orifice from the external gas is given by Equation (15). However, only ωN_w^- of the molecules enter the cavity; the remainder, $(1 - \omega)N_w^-$, recross the surface of the plate. For a steady-state condition the net flux of molecules must be zero. This fact permits writing

$$N_{\text{out}} + (1 - \omega)N_w^- = N_w^-.$$

Substituting from Equations (15) and (21) yields

$$p_{i,d \rightarrow 0} = n_w^- m \sqrt{(RT_w)^+ \sqrt{(RT_w)^-}} \quad (22)$$

This result is valid for $0 \lesssim a \lesssim \infty$ because the dependence upon the transmission probability $\omega(a/d)$ vanishes.

Because the net flux of molecules passing any plane parallel to the plate is zero, Equations (15) and (16) may be equated to give

$$n_w^+ \sqrt{(T_w)^+} = n_w^- \sqrt{(T_w)^-} \quad (23)$$

Using this relation in Equations (17), (20), and (22) there results

$$p_w = \frac{1}{2} m R n_w^+ \sqrt{(T_w)^+} [\sqrt{(T_w)^-} + \sqrt{(T_w)^+}] \quad (24)$$

$$\dot{q} = \frac{n_w^+ m \sqrt{(RT_w)^+} R}{2\sqrt{2\pi}} \left(\frac{\gamma + 1}{\gamma - 1} \right) (T_w^+ - T_w^-) \quad (25)$$

$$p_{i)d \rightarrow 0} = m R n_w^+ / (T_w^+)^{\gamma} / (T_w) . \quad (26)$$

Eliminating n_w^+ , T_w^+ , and T_w^- from Equations (12), (24), (25), and (26) yields

$$\frac{p_{i)d \rightarrow 0}}{p_w} = \frac{2}{\sqrt{\left[1 - \frac{2\sqrt{(2\pi)\dot{q}(\gamma-1)}}{\alpha_w p_{i)d \rightarrow 0}^{\gamma} (RT_w)(\gamma+1)}\right]} + \sqrt{\left[1 - \frac{2\sqrt{(2\pi)\dot{q}(\gamma-1)(1-\alpha_w)}}{\alpha_w p_{i)d \rightarrow 0}^{\gamma} (RT_w)(\gamma+1)}\right]}} . \quad (27)$$

The ratio $p_{i)d \rightarrow 0}/p_w$ is plotted as a function of $\dot{q}(\gamma-1)/[p_{i)d \rightarrow 0}^{\gamma}(RT_w)(\gamma+1)]$ for various values of α_w in Figure 1. Multiplying the abscissa by the ordinate permits plotting $p_{i)d \rightarrow 0}/p_w$ versus $\dot{q}(\gamma-1)/[p_w^{\gamma}(RT_w)(\gamma+1)]$, as shown in Figure 2. Notice that in general neither p_w nor $p_{i)d \rightarrow 0}$ is known from direct measurements. These two pressures represent the two extremes, p_w the pressure that would be indicated for $d \gg \lambda$ (i.e., the true force per unit area on the wall) and $p_{i)d \rightarrow 0}$ the pressure that would be measured by an infinitely small orifice. Therefore, Figures 1 and 2 would prove useful were an iteration technique required.

In order to obtain a suitable expression for \dot{q} , it is necessary to return to the evaluation of n^+ , n^- , T^+ , and T^- . For simplicity, the force between two molecules is assumed to be proportional to the inverse fifth power of the separation distance (i.e., Maxwell molecules). Using the present nomenclature, the results¹⁶ at each plate are

$$\left. \begin{aligned} T_w^- &= (J-1)^2 T_w^+ \\ T_1^+ &= (L+2-J)^2 T_w^+ \\ T_1^- &= L^2 T_w^+ \\ n_w^- &= \frac{n_w^+}{J-1} \\ n_1^+ &= \frac{n_w^+ J}{(L+2-J)(2L+2-J)} \\ n_1^- &= \frac{n_w^+ J}{L(2L+2-J)} \end{aligned} \right\} \quad (28)$$

where

$$L = \sqrt{(T_1^-/T_w^+)} \quad (29)$$

$$J = \frac{[(1+B)(L^4 + 2L^3 + B) + L^2]^{\frac{1}{2}} - (L^3 + 2L^2 - B - 1)}{1 + B - L^2} \quad (30)$$

and $B = (8/15)h/\lambda_w^+$

with $\lambda_w^+ = \lambda(T_w^+, mRn_w^+T_w^+)$.

Using T_w^- , T_1^+ , and T_1^- from Equation (28) in Equations (12) and (13) gives

$$T_w = T_w^+ \left[(J-1)^2 - \frac{J(J-2)}{\alpha_w} \right] \quad (31)$$

and

$$T_1 = T_w^+ \left[(L+2-J)^2 - \frac{(L+2-J)^2 - L^2}{\alpha_1} \right] . \quad (32)$$

Eliminating n_w^+ , n_w^- , T_w^+ , and T_w^- from Equations (20) and (24) and using Equations (28) and (31) gives a theoretical expression for \dot{q} which, being restricted to Maxwell molecules, will be denoted by \dot{q}_t . The result is

$$\dot{q}_t = \frac{p_w \sqrt{RT_w}}{\sqrt{2\pi}} \left(\frac{\gamma+1}{\gamma-1} \right) \frac{(2-J)}{[(J-1)^2 - J(J-2)/\alpha_w]^{1/2}} . \quad (33)$$

This expression for the heat flux between two plates is an exact solution to the basic equations for Maxwell molecules with a two-sided velocity distribution function and is valid over the entire range of density and plate spacings. However, at the lower Knudsen number, based upon plate spacing, the result is only qualitative because the intermolecular potential is more dominant and the velocity distribution function is open to question.

Also, following Liu and Lees¹⁶ it can be established that Equations (27) and (33) are valid at conditions where a mass velocity tangential to the surface exists, so long as the shear stress at the surface is not too large compared to the local pressure. In fact, the abscissa in Figure 1 or 2 is modified with the addition of a term containing the square of the shear stress. Inasmuch as this effect is not the present subject of investigation, it will not be pursued further.

Both to confirm the analysis and to extend knowledge of the predicted effect to conditions where d/λ is arbitrary, an experiment was conducted and will be discussed in more detail in the following section.

4. EXPERIMENTAL APPARATUS AND PROCEDURE

As discussed in an earlier section, the measurements of thermo-molecular pressures in tubes by all previous investigators are wanting in validation, primarily because of failure to make a direct determination of pressure at the tube end which was either hotter or cooler than gage temperature. Also, the effect of tube length never has been adequately determined. Similarly, the investigation of thermo-molecular pressures at orifices by one of the present authors and colleagues¹⁵ is open to criticism because, here again, the heat flux and the pressure outside the orifice were not known from direct measurements.

As part of the present study, the authors constructed the apparatus, shown in Figures 3, 4, and 5, which enables determination of all pressures of interest by direct measurements. The apparatus was designed such that thermo-molecular pressures either at orifices or in tubes can be measured independently and also such that by transient methods the heat-transfer rate to the orifice surface could be measured directly*.

The apparatus was contained in a sealed chamber of controllable atmosphere and consisted essentially of the following:

- (i) An upper or source plate suspended within a guard ring from a force balance.
- (ii) A lower or orifice plate rigidly supported directly beneath the upper plate and containing a total of eighteen orifices of assorted geometry (see Figure 5).
- (iii) Eighteen tubes of assorted diameters and lengths connecting the orifices to a copper block maintained at room temperature by water cooling (see Figure 5).
- (iv) Tabulation and scanner valve connecting the copper blocks to a pressure transducer.
- (v) Electrical resistance heating systems for upper plate, guard ring, and for lower plate with independent controls.
- (vi) A nulling, force balance with external servoamplifiers and recorder with a capability of measuring a difference in pressure above and below the top plate (Knudsen manometer effect) to an accuracy of $\pm 0.2 \mu\text{Hg}$.
- (vii) Differential pressure transducer, MKS Instruments, Inc., Baratron[®] with full-scale ranges of 1, 3, 10, 30, 100, 300, 1000, and 3000 μHg .
- (viii) Pressure scanner valve.
- (ix) Oil-filled manometer graduated in 10^{-3} in. increments.
- (x) Reference vacuum system.
- (xi) Test chamber vacuum pumping system with main valve.
- (xii) Cooling system for lower plate.
- (xiii) Thermocouples as indicated and miscellaneous readout equipment.

Measurement of the thermo-molecular pressure gradient in the tubes was accomplished by heating both plates to an elevated temperature of 644°K and bleeding in a known test gas to a desired pressure level. Because there was no heat transfer between plates, the pressure inside the orifices at the hot ends of the tubes under test should have been equal to that outside the orifices. This was determined by measuring the chamber pressure and then adding or subtracting the difference of pressures above and below

* It should be pointed out that heat-transfer rates and thermo-molecular pressure measurements were not performed simultaneously, since in one case transient methods were used whereas in the other steady state is required.

the top plate, the latter being determined by use of the force balance and known area of the top plate. The pressure existing in the end of the tube terminating in the copper block could be read directly by the transducer connected to the scanner valve, since no temperature gradients existed between the block and transducer.

Measurement of the thermo-molecular pressure across the orifices was accomplished in a similar manner, except with the top plate heated and the bottom plate maintained at room temperature. In that case the pressure just inside the orifice cavity could be assumed equal to that existing at the pressure transducer, because no temperature gradients existed between them. The pressure outside the orifice cavity was again determined by measurement of chamber pressure and the force balance reading. To ascertain the heat flux to the orifice surface, transient temperature readings of the top plate were taken with heater power off. This was done first with the bottom plate heated and then with the bottom plate at room temperature. This difference, together with the known thermal capacity of the top plate, was sufficient to determine the heat flux to the orifice surface.

It should be pointed out that the method of heating the top plate was by radiation from wire heating elements centered in holes drilled through the guard ring and top plate. This was done to minimize the possibility of the heating system exerting a force that was sensed by the balance, thereby giving an erroneous indication.

Another point that should be made is that frequent calibration of the force balance was conducted by application of known weights during the tests and that the pressure transducer was calibrated against the oil manometer each time the chamber pressure was measured.

5. DISCUSSION OF RESULTS

5.1 Thermo-Molecular Pressure in Tubes

To determine the effect of thermo-molecular pressures in tubes, the pressure and temperature were measured at each end of tubes of varying geometries, as given in Figure 5. The temperatures were measured directly using Chromel[®]-Alumel[®] thermocouples. The pressure difference between that existing at the cold end of the tube and the ambient pressure in the tank was measured using the differential pressure transducer. The most sensitive range was $\pm 1 \mu\text{Hg}$, full scale. The difference in the tank pressure and that existing at the hot end of the tube (i. e., between the plates) was measured by the differential balance. The pressure in the tank was measured directly, using the pressure transducer with one side connected to a reference pressure of approximately $0.01 \mu\text{Hg}$, as discussed in a previous section.

In Section 3 it was shown that the quantity $\sqrt{\{(dT/dp)(p/2T)\}}$ can be expected to be an important parameter for purposes of correlating the data. For convenience, let

$$X = \sqrt{\left(\frac{dT}{dp} \frac{p}{2T}\right)} \quad (34)$$

Now from Equations (5) and (7) it is seen that X can be expected to be a linear function of the inverse Knudsen number in both the slip flow and the near free molecular

regimes. This result is valid only for infinitesimal pressure and temperature differences. Since for all practical applications a finite temperature difference will exist, it is desirable to generalize the above parameter to include arbitrary differences of temperature. Of course, the differential expression could be integrated if the variations of temperature with inverse Knudsen number were known. However, it would be far easier if this integration could be avoided.

The first modification that one might consider is to replace the differential with finite differences and the pressure and temperature with mean values. It can be shown (Arney and Bailey¹⁴) that this approach fails to give the correct free molecule limit of unity except for vanishingly small temperature differences. A parameter that reduces to the differential parameter and also gives the correct free molecule limit is

$$X = \sqrt{\left\{ \frac{1 - \sqrt{T_1/T_2}}{1 - p_1/p_2} \right\}^2}. \quad (35)$$

First, note that, when $p_1/p_2 = \sqrt{T_1/T_2}$, X reduces to unity, satisfying the free molecule condition. Then consider the limit as T_1 approaches T_2 .

Let

$$T_1 = T - \Delta T, \quad T_2 = T$$

and

$$p_1 = p - \Delta p, \quad p_2 = p.$$

Then

$$T_1/T_2 = (T - \Delta T)/T = 1 - \frac{\Delta T}{T}$$

and likewise

$$p_1/p_2 = \left(1 - \frac{\Delta p}{p} \right).$$

For $\Delta T/T_2 \ll 1$, the following approximation can be written

$$\sqrt{T_1/T_2} = 1 - \frac{\Delta T}{2T}$$

and X becomes

$$\sqrt{\frac{1 - \left(1 - \frac{\Delta T}{2T} \right)}{1 - \left(1 - \frac{\Delta p}{p} \right)}} = \sqrt{\frac{\frac{\Delta T}{2T} p}{\Delta p}}.$$

Therefore, Equation (35) is a satisfactory generalization of Equation (34) insofar as the free molecule and small-temperature-difference limits are concerned. It remains to be seen if the experimental data can be correlated using this generalized parameter.

The theoretical result relating X to the inverse Knudsen number, as has been pointed out, is valid only for infinitesimal temperature differences. Likewise the inverse Knudsen number in turn is a function of the local pressure and temperature. For any practical application it would be desirable to relate the thermo-molecular effect to conditions that may be known, such as those at the end of the tube where the pressure is measured. Like the parameter X , the inverse Knudsen number can also be generalized. To do that, let

$$Z = \left(\frac{T_1}{T_2} \right)^s \frac{1}{\text{Kn}} . \quad (36)$$

Note that Z is a quantity that reduces to $1/\text{Kn}_1$ in the limit of T_1 , approaching T_2 . Because the proof of any correlation parameter rests on its ability to reduce the apparent randomness of the experimental data, the data were plotted as shown in Figures 6 through 9, using $s = 2/3$. This value was required in order to reduce data for various temperature ratios to a single curve. The values of Z were calculated using the definition of mean free path given in Equation (37), viz.,

$$\lambda(T,p) = \frac{16}{5\sqrt{2\pi}} \frac{\mu(T)}{p} \sqrt{RT} , \quad (37)$$

or

$$\lambda(T,p) = \frac{T}{p} f(T) ,$$

where $f(T)$ is given in Figure 10 for various gases. This definition of mean free path is used throughout this discussion.

Notice that the results in Figures 6 through 9 appear to be linear over almost the entire range of Z , with a slope of approximately 0.275 for the higher values of Z (i.e., the slip flow regime).

Figures 11 through 14 more clearly show the behavior of the data in the free molecule and the transitional regimes. It appears that at $X = 0$ a slope of approximately unity is approached, which agrees with Equation (7). Notice that the results for all gases and tubes investigated reduce to essentially the same curve. An empirical equation that seems to fit the experimental data throughout the entire range of Knudsen number for all gases investigated is

$$\sqrt{\frac{1 - (T_1/T_2)^{0.5}}{1 - (p_1/p_2)}} = 1 + 0.275(\text{Kn}_1)^{-1}(T_1/T_2)^{2/3} + \frac{0.625(\text{Kn}_1)^{-1}(T_1/T_2)^{2/3}}{1 + 24.0[(\text{Kn}_1)^{-1}(T_1/T_2)^{2/3}]^2} . \quad (38)$$

This result is based upon data for which $0.5 \lesssim T_1/T_2 \lesssim 2$.

Equation (38) is shown in Figures 6 through 9 and 11 through 14 as the solid curve. In general the subscripts 1 and 2 refer to any two points in a circular tube. In practice the subscript 1 refers to the end where the pressure is measured and the temperature is known, whereas subscript 2 refers to the point where the pressure is desired and the temperature known.

A single exception to the above correlation is tube number 18 (see Figure 5) which has $l/r \simeq 0$. Data from this tube are shown with a flag in Figures 6 through 9 and 11 through 14. This discrepancy possibly represents an effect of length on the thermo-molecular pressure. However, this problem is usually of academic interest, since normally $l/d \gg 1$, and the effect seems to be independent of the length-to-diameter ratio for $l/d \gtrsim 1$.

5.2 Heat Transfer

Although this investigation is not primarily concerned with the heat transfer between parallel plates, in the present case this is an important parameter related to the thermo-molecular pressure effect at orifices. Heat-transfer measurements were made for two reasons. First, since the theory for the thermo-molecular pressures for small orifices is based upon the theory of Liu and Lees, the measurement of heat flux between the two plates could be compared to that predicted in Reference 16, thereby obtaining an idea of the applicability of the theory to the present problem. Secondly, because heat transfer at low pressures is a strong function of the thermal accommodation coefficient, the value of α could be determined to use in the equation for the thermo-molecular pressure effect at an orifice.

As discussed earlier, the heat transfer was determined using a transient technique. The total heat loss from the top and bottom surfaces of the top plate was measured with the bottom plate approximately at room temperature ($\simeq 311^\circ\text{K}$) and the top plate at 644°K . The heat loss from the top surface was then determined with both plates at a temperature of 644°K . Both of these measurements were taken with various pressures existing between the plate ($0 < p_w \lesssim 1000 \mu$) for the four gases tested and for plate spacings of 0.041 and 0.138 in. The difference between these two measurements at a given pressure represents the total net heat exchange between the upper and the lower plates. The value of the heat transfer at $p_w \simeq 0$ represents the net radiation transfer between the plates. Since the radiation is independent of pressure over the pressure range investigated, this vacuum value was subtracted from the results at finite pressures. This final heat transfer is that due to the gas molecules between the two plates. These results for $p_w \lesssim 100 \mu$ are shown in Figures 15 through 18 for two plate spacings and four gases. A value of the accommodation coefficient was chosen that would best fit Equation (33) to the experimental data at small values of the inverse Knudsen number (i.e., near free molecule regime). Values of α obtained in this manner for hydrogen, helium, nitrogen, and argon were 0.42, 0.51, 0.79, and 0.83, respectively. It can be shown that the theory of Liu and Lees will converge to the correct free molecule limit, which gives confidence in the determination of the thermal accommodation coefficient in this manner. However, at higher pressure the theory over-estimates the transfer of heat between parallel plates.

At large values of the inverse Knudsen number, i.e., the continuum regime, the heat flux is given by the Fourier heat conduction law

$$\dot{q}_c = -k \frac{dT}{dy} \quad (39)$$

Since the heat flux is constant at any station between the plates, we may integrate from the bottom plate to the top plate to obtain

$$\dot{q}_c(y_w - y_1) = - \int_{T_w}^{T_1} k(T) dT$$

or

$$\dot{q}_c = \frac{-1}{h} \int_{T_w}^{T_1} k(T) dT, \quad (40)$$

where $(y_w - y_1)$ has been replaced by the plate spacing h .

The experimental data seem to be approaching the continuum heat flux given by Equation (40). In order to better see this, the experimental data for $0 < p_w < 1000 \mu$ were plotted using the parameter $[1 - \dot{q}/\dot{q}_t]/[1 - \dot{q}_c/\dot{q}_{t,c}]$. A value of zero indicates complete agreement with the rarefied-flow theory; on the other hand, a value of 1 signifies that the continuum limit has been reached. The data were plotted as a function of the inverse Knudsen number, as shown in Figure 19. The scatter of the data may at first be misleading since the heat-transfer parameter tends to amplify any error in the data. Almost all the data are within $\pm 5\%$ of the mean. In fact the discrepancy between the theory at high densities and the continuum value for the heat flux is never greater than about 20% for hydrogen, helium, and nitrogen and 11% for argon. The basic cause of this disagreement lies in the fact that the theory is based upon a non-essential but simplifying assumption that the force of repulsion between molecules is proportional to the inverse fifth power of their distance of separation (i.e., Maxwellian molecules).

The continuum limit for the theory obtained by substituting $B \rightarrow \infty$ in Equations (30), (33), and (37) becomes

$$\dot{q}_{t,c} = - \frac{15}{32} \frac{(\gamma + 1)R\mu_w}{(\gamma - 1)h} \left(\frac{T_1 + T_w}{T_w} \right) (T_1 - T_w). \quad (41)$$

The empirical curve in Figure 19, which seems to be representative of the data, is given by the equation

$$\frac{1 - \dot{q}/\dot{q}_t}{1 - \dot{q}_c/\dot{q}_{t,c}} = \frac{(1/\text{Kn}_{w,w,h})^{3/2}}{3 + (1/\text{Kn}_{w,w,h})^{3/2}}. \quad (42)$$

5.3 Thermo-Molecular Pressure at Orifices

The indicated pressure p_i was measured for various sizes and geometries of orifices, as shown in Figure 5. The bottom plate containing these orifices was subjected to varying fluxes of energy by heating the upper plate to a temperature T_1 . Two plate spacings, h , were used. Four gases, hydrogen, helium, nitrogen, and argon, were tested at various pressures. The results were normalized and made dimensionless by

plotting \bar{p} versus $1/\text{Kn}_{w,i,d}$, where

$$\bar{p} = \frac{p_i - p_{i,d \rightarrow 0}}{p_w - p_{i,d \rightarrow 0}} \quad (43)$$

The true force per unit area p_w on the lower plate was determined from the force balance. The limit $p_{i,d \rightarrow 0}$ was determined from Equation (27) (as shown in Figure 2), using the result of the heat flux measurements as given by Equation (42), with \dot{q}_t , \dot{q}_c , and $\dot{q}_{t,c}$ given by Equations (33), (40), and (41), respectively. The results for circular orifices using hydrogen and helium, nitrogen and argon are shown in Figures 20 through 23.

The data points in Figures 20 through 23 are symbolized according to orifice length, a . The open symbols are for $0.005 \leq a \leq 0.014$ in., the half dark for $a = 0.1$ in., and the dark for $2.5 \leq a \leq 6.0$ in. In general, it appears that the data for the short orifices may fall slightly below the data for the long orifices. However, it is assumed that any length effect, if indeed one exists, is small and will be neglected in the remainder of this paper.

Notice, however, that there is a systematic shift of the data to the left with increasing molecular weight M of the gas. This function of M varies as approximately $M^{1/8}$. An empirical equation that seems representative of the data for hydrogen, helium, nitrogen, and argon over the entire range of inverse Knudsen number is

$$\bar{p} = \frac{0.3148(M^{1/8}/\text{Kn}_{w,i,d})^{1/2} + 0.01478(M^{1/8}/\text{Kn}_{w,i,d})^2}{1.0 + 0.3148(M^{1/8}/\text{Kn}_{w,i,d})^{1/2} + 0.01478(M^{1/8}/\text{Kn}_{w,i,d})^2} \quad (44)$$

Orifices 16 and 17 in Figure 5 are circular slots. While admittedly this geometry is not often used in practice, it was chosen because of the ease of incorporation into the lower plate. It was also felt that, because the radius of curvature was large compared to the slot width (7.14 and 17.9 times), the results would be essentially the same as for a straight slot. Also, the results should compare with an infinite slot, since there is no end effect. The results for the slots are shown in Figure 24, with the same parameters as used for the circular orifice, except that the inverse Knudsen number is based upon the slot width as the characteristic dimension. The empirical curve is given by

$$\bar{p} = \frac{0.4485(M^{1/8}/\text{Kn}_{w,i,g})^{1/2} + 0.0608(M^{1/8}/\text{Kn}_{w,i,g})^2}{1.0 + 0.4485(M^{1/8}/\text{Kn}_{w,i,g})^{1/2} + 0.0608(M^{1/8}/\text{Kn}_{w,i,g})^2} \quad (45)$$

The constants in Equation (45) were influenced somewhat by those in Equation (44), since the empirical curves are relatively insensitive to the magnitude of the constant in the squared term. This flexibility permits the equations for the slots to reduce to the equations for the circular orifices if an effective diameter is defined such that

$$d_{\text{eff}} = 2.03g \quad (46)$$

This value of $d_{\text{eff}}/g = 2.03$ is close to the ratio of 2.0 corresponding to the use of the hydraulic radius of an infinite straight slot for d_{eff} . Slightly smaller values of the hydraulic radius are obtained for the circular slots used in the experiment. Offhand there seems to be no means why a hydraulic radius should be applied to the present problem, although the comparison is possibly of interest.

6. APPLICATION OF RESULTS

In the previous sections the results of theory and experiment for both the thermo-molecular pressure effect in tubes and at orifices have been presented without much regard for the practical applications of results. This section will include most pertinent results from previous sections, as well as examples of their use. The calculation of all Knudsen numbers will be based upon the mean free path defined by Equation (37) and plotted in Figure 10.

6.1 Tube Effect

The results of the thermo-molecular pressure effect in tubes, both theoretical and experimental, are given in Equation (38):

$$\sqrt{\left[\frac{1 - (T_1/T_2)^{0.5}}{1 - p_1/p_2} \right]} = 1 + 0.275(\text{Kn})^{-1}(T_1/T_2)^{2/3} + \frac{0.625(\text{Kn})^{-1}(T_1/T_2)^{2/3}}{1 + 24.0[(\text{Kn})^{-1}(T_1/T_2)^{2/3}]^2} \quad (38)$$

The subscript 1 refers to the end where the pressure is measured or known, and the subscript 2 refers to a point where the temperature is known and the pressure is desired. This equation is based upon data for

$$0.5 \lesssim T_1/T_2 \lesssim 2.$$

If the temperature ratio is outside this range, Equation (38) should be used with caution. A more accurate method would be to use the differential form of Equation (38) where $T_1 \rightarrow T_2$, that is

$$\sqrt{\left[\frac{dT}{dp} \frac{p}{2T} \right]} = 1 + \frac{0.275}{\text{Kn}} + \frac{0.625}{\text{Kn}(1 + 24/\text{Kn}^2)} \quad (47)$$

Numerical integration gives

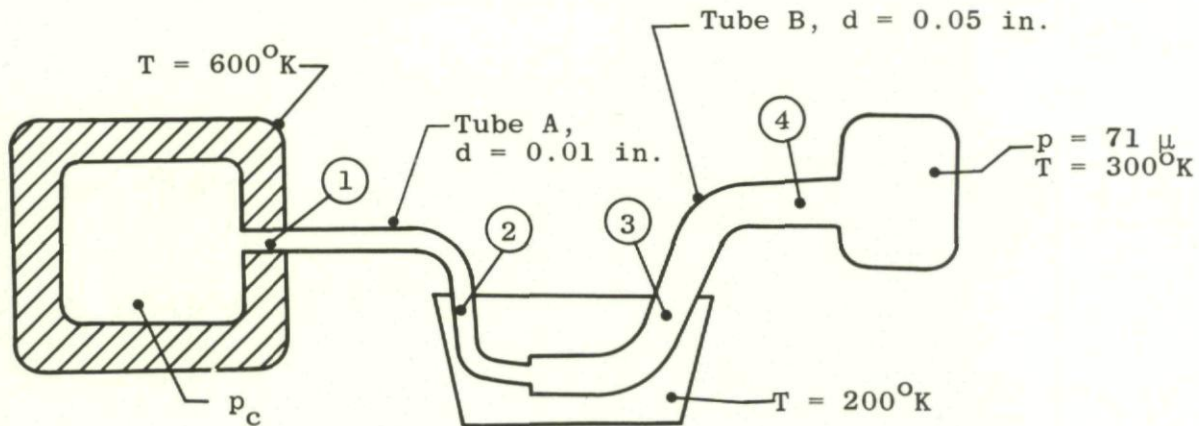
$$p_2 = p_1 + \int_{T_1}^{T_2} \frac{dp}{dT} dT.$$

To illustrate the use of Equation (38), the following example will be considered:

Example I

A 0.01 in. diameter tube connects a low pressure chamber heated to 600°K and a cold trap maintained at 200°K. At the cold trap the tube diameter changes to 0.05 in. and

hence connects to a pressure-measuring device at room temperature (300°K). The pressure indicated by the measuring device is $71\ \mu\text{Hg}$. The entire system contains nitrogen. What is the pressure p_c in the heated chamber?



It will be necessary to use Equation (38) twice because tubes of two sizes with temperature gradients are involved. Note first that

$$p_1 = p_c, \quad p_2 = p_3, \quad \text{and} \quad p_4 = 71\ \mu\text{Hg},$$

because the components between these equal pressures are at uniform temperatures. From Figure 10, at 300°K for nitrogen

$$\frac{\lambda p}{T} = 0.00665 \frac{\text{in. } \mu\text{Hg}}{^{\circ}\text{K}}$$

or

$$\lambda_4 = \frac{(0.00665)(300)}{71} = 0.0281 \text{ in.}$$

Therefore

$$\text{Kn}_4 = 0.0281/0.05 = 0.562$$

$$T_4 = 300^{\circ}\text{K}$$

$$T_3 = 200^{\circ}\text{K}$$

Equation (38) becomes, for tube B,

$$\sqrt{\left[\frac{1 - (300/200)^{1/2}}{1 - (71/p_3)} \right]} = 1 + \frac{0.275}{0.562} \left(\frac{300}{200} \right)^{2/3} + \frac{0.675}{0.562} \left(\frac{300}{200} \right)^{2/3} \frac{1}{1 + 24(3/2)^{3/2} (0.562)^{-2}}$$

Solving for p_3 gives

$$p_3 = 65.6\mu = p_2 .$$

Again, using Figure 10 for $T = 200^\circ\text{K}$ gives $\text{Kn}_2 = 1.829$. Using Equation (38) on tube A gives

$$\frac{1 - (200/600)^{1/2}}{1 - (65.6/p_1)} = 1 + \frac{0.275}{1.8292} \left(\frac{200}{600}\right)^{2/3} + \frac{0.675}{1.8292} \left(\frac{200}{600}\right)^{2/3} \frac{1}{1 + 24(200/600)^{2/3}(1.8292)^{-2}}$$

or

$$p_1 = 97.7\mu = p_c ,$$

which is the required pressure.

6.2 Orifice Effect

The results of the thermo-molecular pressure effect at orifices are given by Equations (27), (43), and (44). These three equations contain the generally unknown quantities $p_w, p_{i,d \rightarrow 0}$, and \bar{p} . Equation (44) can be used to yield \bar{p} directly. However, difficulty arises when an attempt is made to solve for, say, p_w from Equations (27) and (43). Eliminating $p_{i,d \rightarrow 0}$ from these two equations gives

$$\begin{aligned} & 4(2\bar{p} - 1) + 8 \frac{p_i}{p_w} \bar{p} \left[-1 + \sqrt{(2\pi)\kappa} \left(\frac{1}{\alpha} - \frac{1}{2} \right) (1 - \bar{p}) \right] + \\ & + 2 \left(\frac{p_i}{p_w} \right)^2 \left[2 - \pi\kappa^2 (\bar{p}^2 + 2\bar{p} - 1) - 4\sqrt{(2\pi)\kappa} \left(\frac{1}{\alpha} - \frac{1}{2} \right) (1 - \bar{p}) \right] + \\ & + 8\pi\kappa^2 \left(\frac{p_i}{p_w} \right)^3 \bar{p} \left[1 - \frac{\sqrt{(2\pi)\kappa}}{2} \left(\frac{1}{\alpha} - \frac{1}{2} \right) (1 - \bar{p}) \right] + \\ & + 4\pi\kappa^2 \left(\frac{p_i}{p_w} \right)^4 \left[-1 + \frac{\pi\kappa^2}{4} \bar{p}^2 + \sqrt{(2\pi)\kappa} \left(\frac{1}{\alpha} - \frac{1}{2} \right) (1 - \bar{p}) \right] - \\ & - 2\pi^2\kappa^4 \left(\frac{p_i}{p_w} \right)^5 \bar{p} + \pi^2\kappa^4 \left(\frac{p_i}{p_w} \right)^6 = 0 , \end{aligned} \quad (48)$$

where $\kappa = \dot{q}(\gamma - 1)/(p_i \sqrt{RT_w})(\gamma + 1)$.

This equation is a sixth degree polynomial in the unknown p_i/p_w . Equation (48) is plotted in Figure 25 with p_i/p_w as a function of κ for various values of the parameters α and $M^{1/8}/\text{Kn}_{w,i,d}$. For the usual application of Equation (48) or Figure 25 the variables γ , p_i , R , T_w , M and d are known. However, α and \dot{q} must be determined independently from experimental measurements, theory or available data. For a discussion of thermal accommodation coefficient see the review articles by Hurlbut²¹ or Wachman²². An example will be considered in order to show how the correction at an orifice is made.

Example II

A 1/8 in. diameter circular orifice in a plane surface is exposed to helium at an elevated temperature. The surface is maintained at room temperature ($T_w = 300^\circ\text{K}$). The pressure measured by a sensing device, also at room temperature, connected to the orifice by a 0.25 in. diameter tube is 326μ . The energy flux to the wall is $2.39 \text{ Btu/ft}^2 \text{ sec}$. It is known that the thermal accommodation coefficient of the gas/wall interface is 0.3. What is the true pressure on the surface?

For helium, $\gamma = 1.667$, $M = 4.003$, and $R = 2.238 \times 10^4 \text{ ft}^2/(\text{sec}^2 \text{ }^\circ\text{K})$. The pressure inside the orifice is also 326μ , since there is no temperature gradient along the 0.25 in. tube. From Figure 6, for $T = 300^\circ\text{K}$,

$$\frac{\lambda p}{T} = 0.0202 .$$

Therefore,

$$\lambda(p_i, T_w) = \frac{(0.0202)(300)}{326} = 0.0185 \text{ in.} ,$$

giving

$$\text{Kn}_{w, i, d} = \frac{0.0185}{0.125} = 0.148$$

$$\frac{M^{1/8}}{\text{Kn}_{w, i, d}} = \frac{(4.003)^{1/8}}{0.148} = 8.0$$

$$\dot{q} = -2.39 \frac{\text{Btu}}{\text{ft}^2 \text{ sec}} \left(778 \frac{\text{ft lbf}}{\text{Btu}} \right) = -1860 \frac{\text{ft lbf}}{\text{ft}^2 \text{ sec}}$$

$$p_i = (326\mu) \left(2.784 \times 10^{-3} \frac{\text{lbf}}{\mu \text{ft}^2} \right) = 0.9075 \frac{\text{lbf}}{\text{ft}^2} .$$

Solving for κ

$$\kappa = \frac{(-1860)(0.667)}{(0.9075)(2.238 \times 10^4)^{1/2} (300)^{1/2} (2.667)} = -0.198 .$$

Using Figure 25 with $m^{1/8}/\text{Kn}_{w, i, d} = 8.0$, $\kappa = -0.198$ and $\alpha = 0.3$ gives

$$p_i/p_w = 0.784$$

or

$$p_w = \frac{326\mu}{0.784} = 416\mu .$$

Thus the true pressure is almost 20% different from the measured pressure.

It is hoped that these examples will serve to illustrate the method of making thermo-molecular pressure correction and will also show the magnitude of correction that may be encountered.

ACKNOWLEDGMENT

The authors have benefited from the aid of several persons. Mrs Betty M. Majors, Mr R.F. Armstrong, and Mr K. Rawlings deserve particular recognition and sincere thanks for assistance with experiments and computations.

This work is based on research sponsored by the Arnold Engineering Development Center, Air Force Systems Command, US Air Force, under Contract AF 40(600)-1200. Further reproduction to satisfy needs of the US Government is authorized.

REFERENCES

1. Knudsen, Martin *Eine Revision der Gleichgewichtsbedingung der Gase. Thermische Molekularstromung.* Annalen der Physik, Vol. 31, 1910, pp. 205-229.
2. Bailey, A.B.
Boylan, D.E. *Proceedings of the 1962 Heat Transfer and Fluid Mechanics Institute.* (Edited by F.E. Ehlers, J.J. Kauzlarich, C.A. Sleicher, Jr, and R.E. Street) Stanford University Press, Stanford, California, 1962, pp. 62-75.
3. Bailey, A.B. *Further Experiments on Impact-Pressure Probes in a Low-Density, Hypervelocity Flow.* Arnold Engineering Development Center, AEDC-TDR-62-208, November 1962.
4. Potter, J.L.
Bailey, A.B. *Pressures in the Stagnation Regions of Blunt Bodies in Rarefied Flow.* Journal of the American Institute of Aeronautics and Astronautics, Vol. 2, 1964, pp. 743-745.
5. Kennard, Earle H. *Kinetic Theory of Gases.* McGraw-Hill, New York and London, 1938, pp. 327-333.
6. Neumann, C. Bericht der Koniglich Sachsen Gesellschaft der Wissenschaft. Mathem. Phys Kl., Vol. 24, 1872, p. 49.
7. Feddersen, W. *Über Thermodiffusion von Gasen.* Poggendorf Annalen (now Annalen der Physik), Vol. 148, 1873, p. 302.
8. Reynolds, Osborne *On Certain Dimensional Properties of Matter in Gaseous State.* Royal Society of London, Philosophical Transactions, Vol. 170, Part 2, 1879, pp. 727-845.
9. Maxwell, J. Clerk *On Stresses in Rarefied Gases Arising from Inequalities of Temperature.* Royal Society of London, Philosophical Transactions, Vol. 170, 1879, pp. 231-256.
10. Knudsen, Martin *Thermischer Molekulardruck der Gase in Röhren.* Annalen der Physik, Vol. 33, 1910, pp. 1435-1448.
11. Knudsen, Martin *Thermischer Molekulardruck in Röhren.* Annalen der Physik, Vol. 83, 1927, pp. 797-821.
12. Tompkins, F.C.
Wheeler, D.E. *The Correction for Thermo-Molecular Flow.* Transactions of the Faraday Society, Vol. 29, November 1933, pp. 1248-1254.
13. Howard, Weston M. *An Experimental Investigation of Pressure Gradients due to Temperature Gradients in Small Diameter Tubes.* Guggenheim Aeronautical Laboratory, California Institute of Technology, Pasadena, California, Memorandum No. 27, June 10, 1955.

14. Arney, G.D.
Bailey, A.B. *Addendum to Investigation of the Equilibrium Pressure along Unequally Heated Tubes.* Arnold Engineering Development Center, AEDC-TDR-62-188, October 1962.
15. Potter, J.L.
et al. *Rarefied Gas Dynamics.* (Edited by J.H. de Leeuw) Vol. 2, Academic Press, New York, 1966, pp. 175-194.
16. Liu, Chung-Yen
Lees, L. *Rarefied Gas Dynamics.* (Edited by L. Talbot), Academic Press, New York, 1961, pp. 391-428.
17. Lees, L. *A Kinetic Theory Description of Rarefied Gas Flows.* Guggenheim Aeronautical Laboratory, California Institute of Technology, Hypersonic Research Project Memorandum No. 51, December 15, 1959.
18. de Leeuw, J.H.
Rothe, D.E. *A Numerical Solution for the Free-Molecule Impact-Pressure Probe Relations for Tubes of Arbitrary Length.* University of Toronto Institute of Aerophysics, UTIA Report 88, December 1962.
19. Clausing, P. *Ueber die Stremung sehr verduennter Gase durch Roehren von beliebiger Laenge.* Annalen der Physik, Vol. 12, 1932, p. 961.
20. Present, R.D. *Kinetic Theory of Gases.* McGraw-Hill, New York, 1958, p. 22.
21. Hurlbut, F.C. *Rarefied Gas Dynamics.* (Edited by C.L. Brundin) Vol. 1, Academic Press, New York, 1967, pp. 1-34.
22. Wachman, Harold Y. *American Rocket Society Journal*, Vol. 32, No. 1, January 1962, pp. 2-12.

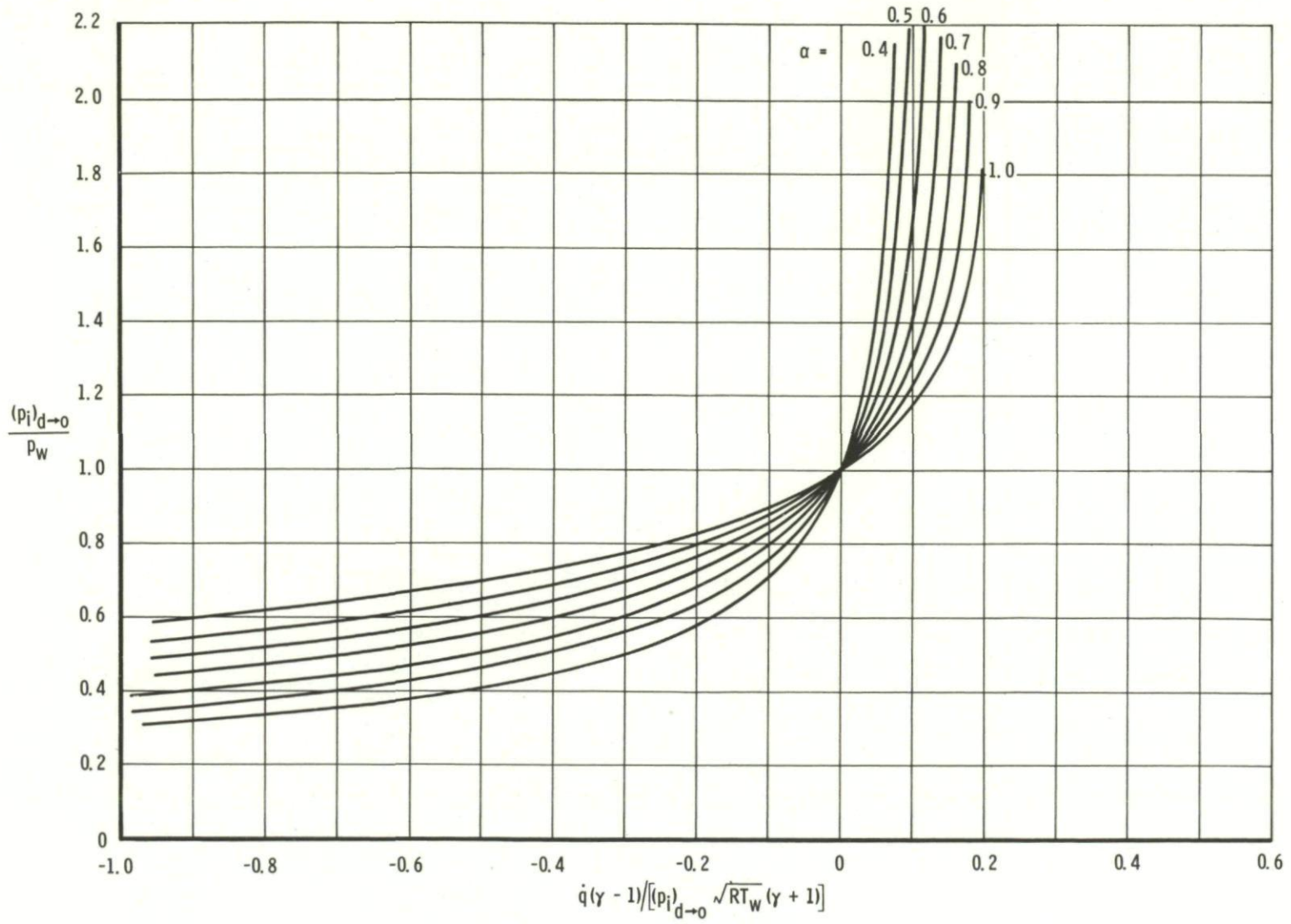


Fig. 1 Plot of Equation (27)

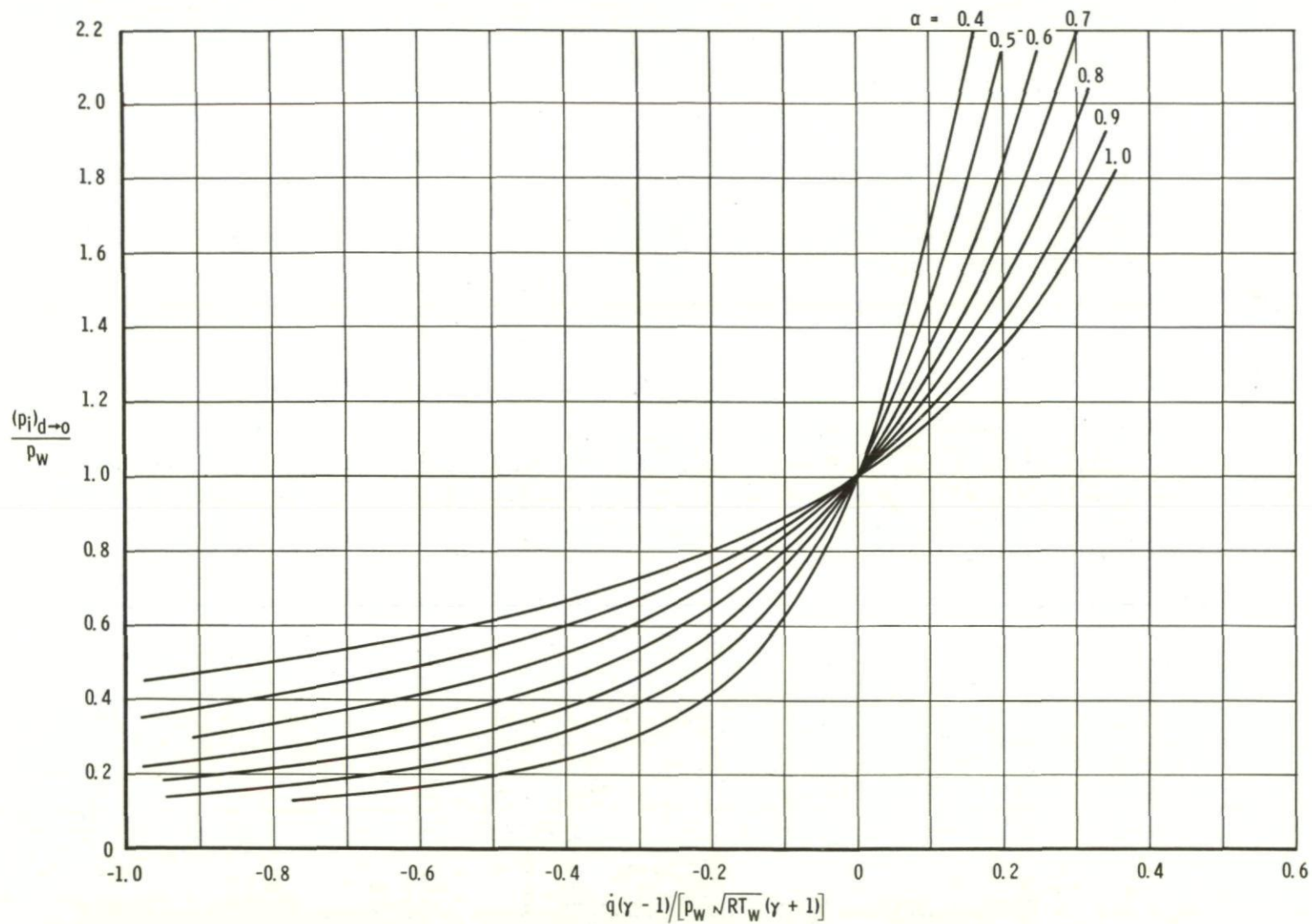


Fig. 2 Plot of modified Equation (27)

- NOTES: 1. Eighteen orifices of different geometry in bottom plate are connected to pressure instrumentation via sections of tubing of assorted sizes and lengths.
2. The symbol \cup denotes a thermocouple.

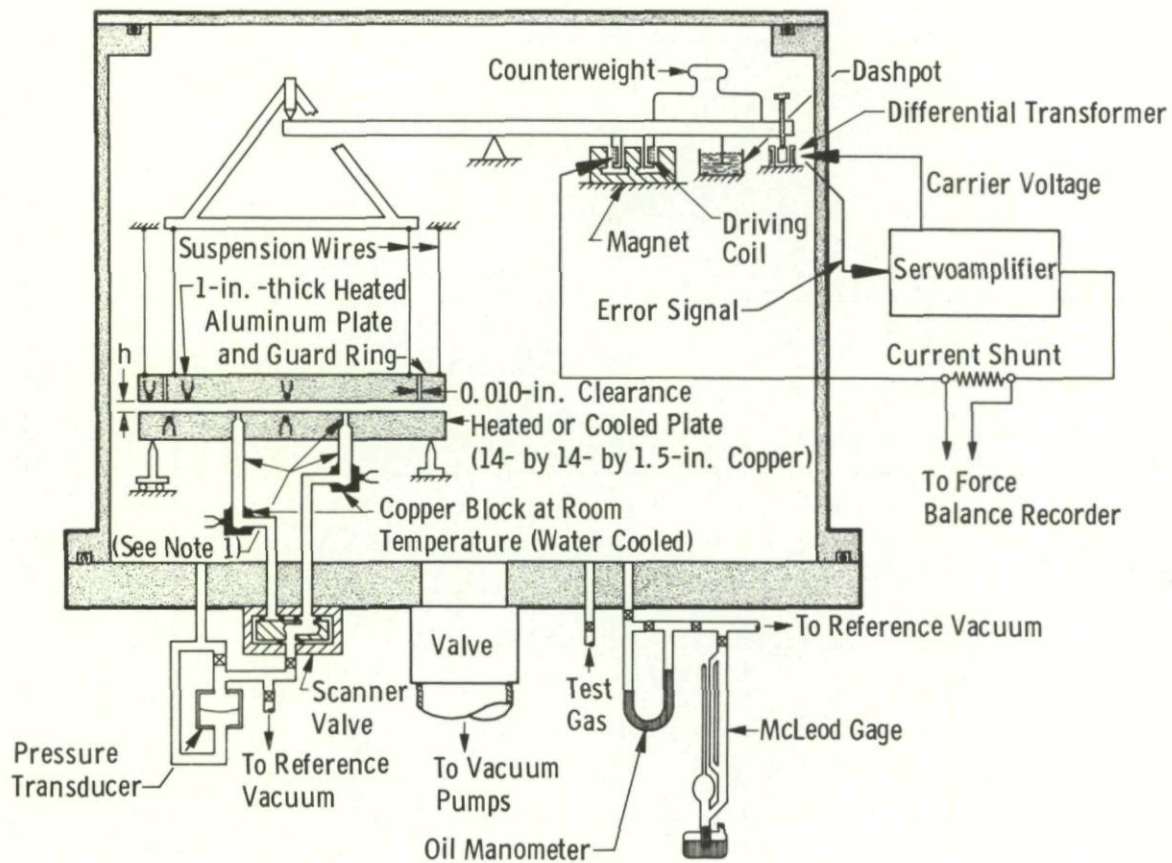


Fig. 3 Sketch of apparatus

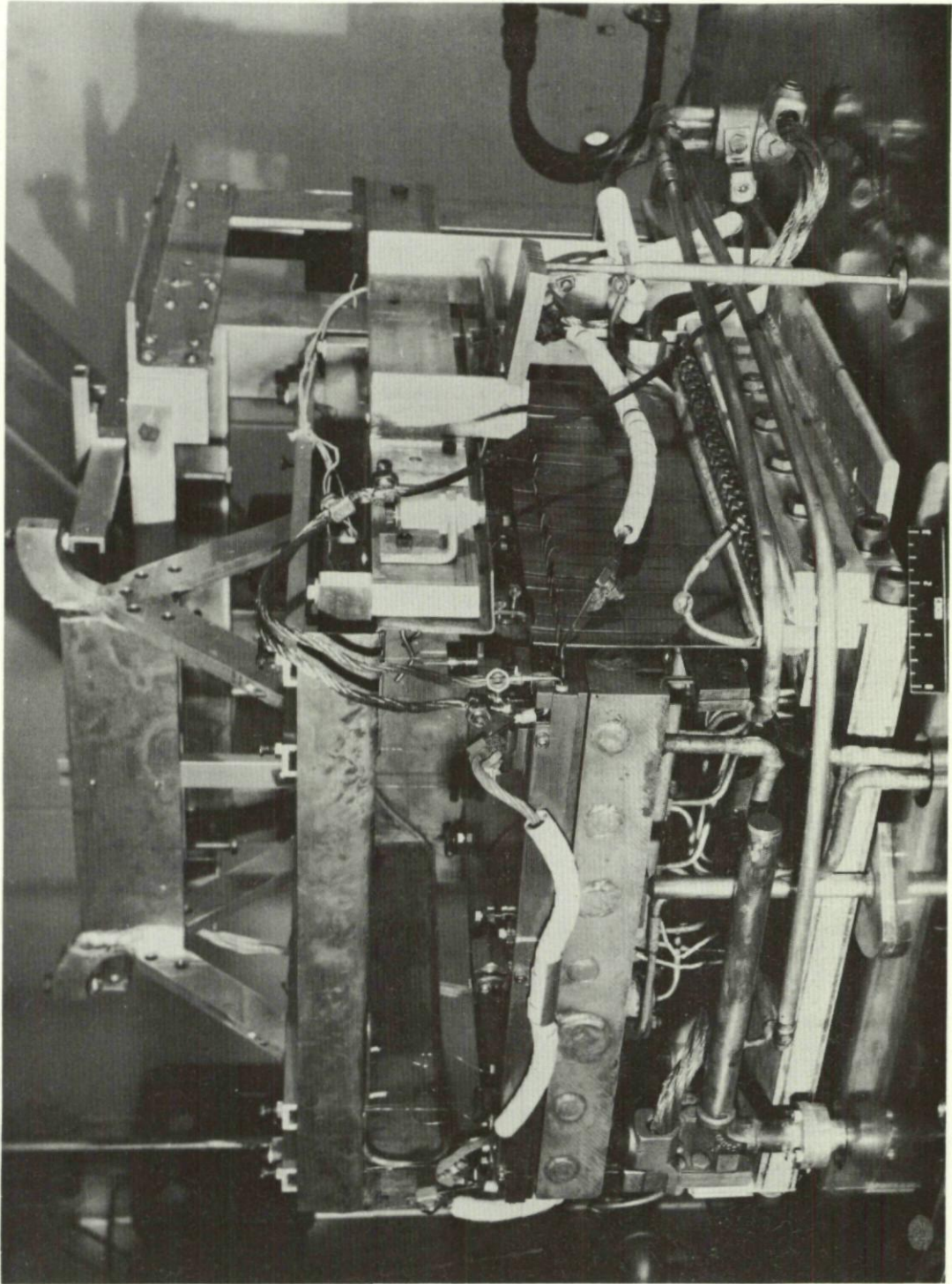
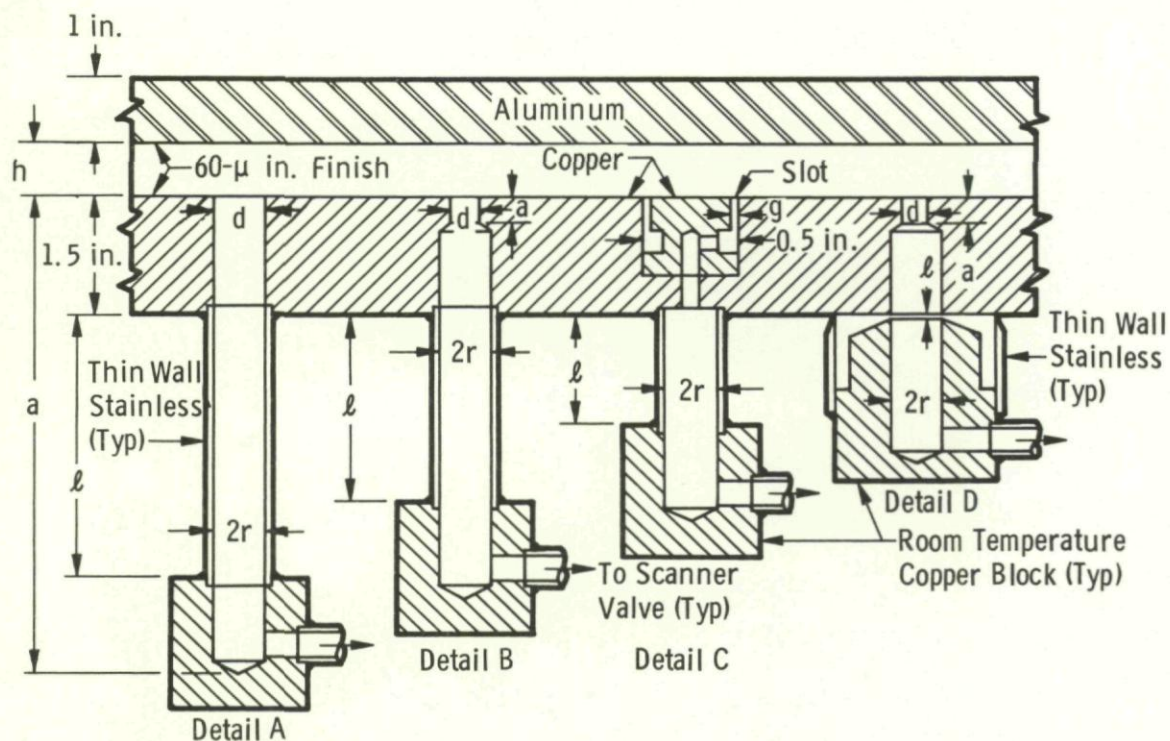


Fig. 4 Photograph of apparatus



SCHEDULE OF DIMENSIONS IN INCHES						
No.	Detail	2r	l	d	a	g
1	A	0.035	1.0	0.035	3.0	
2		0.045	0.5	0.045	2.5	
3		0.066	4.0	0.067	6.0	
4		0.089	1.0	0.089	3.0	
5		0.1475	4.0	0.147	6.0	
6		0.180	4.0	0.180	6.0	
7		0.311	4.0	0.311	6.0	
8		0.436	1.0	0.436	3.0	
9	B	0.1475	0.5	0.0135	0.100	
10			1.0	0.015	0.010	
11			1.0	0.0292	0.100	
12			0.5	0.035	0.005	
13		0.311	0.5	0.089	0.100	
14		0.311	1.0	0.180	0.014	
15		0.436	4.0	0.180	0.014	
16	C	0.035	4.0			0.014
17	C	0.035	0.5			0.035
18	D	0.436	→0	0.180	0.100	

Fig.5 Tube and orifice schedule

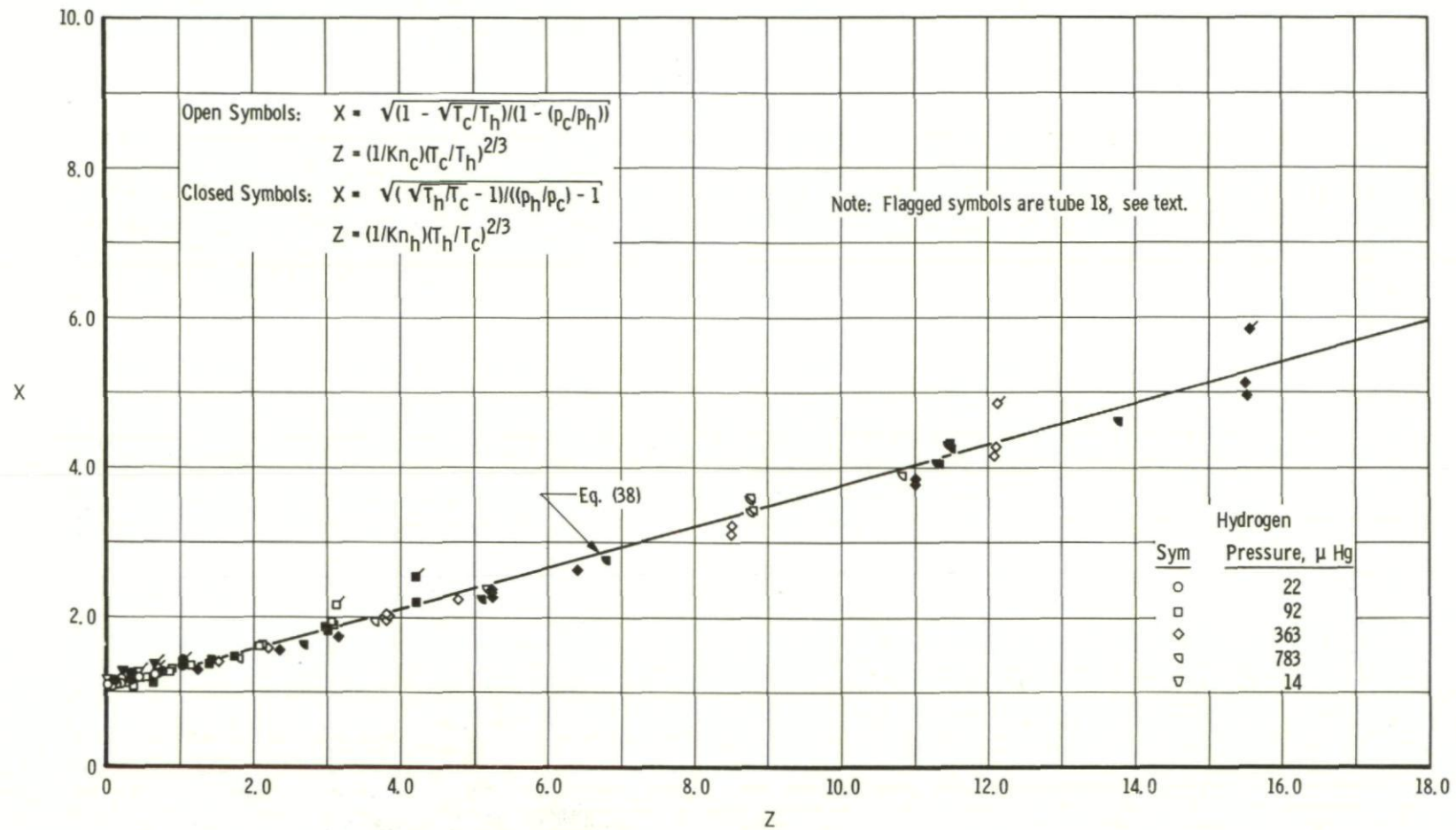


Fig. 6 Slip flow results for tubes using hydrogen

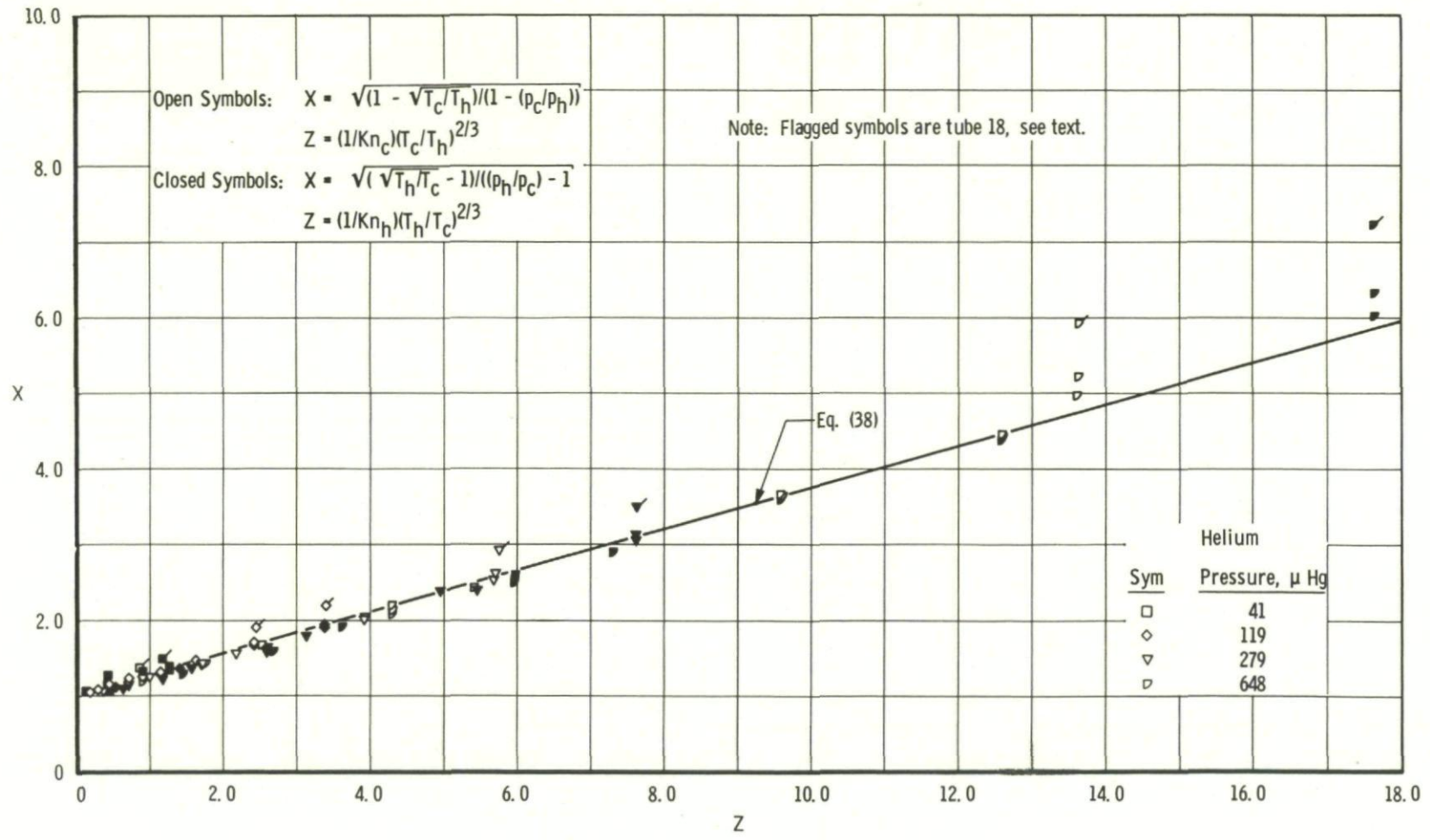


Fig.7 Slip flow results for tubes using helium

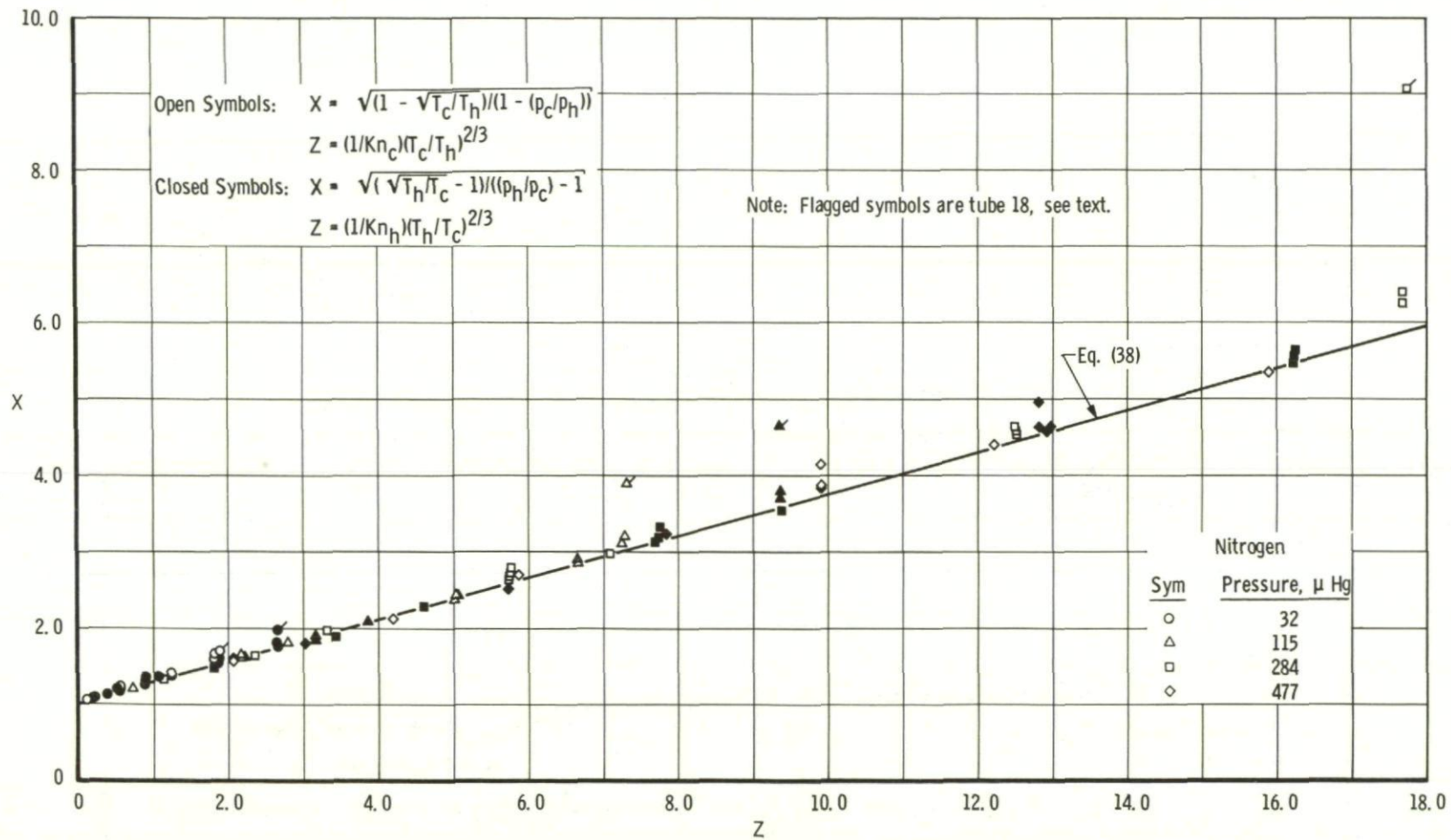


Fig.8 Slip flow results for tubes using nitrogen

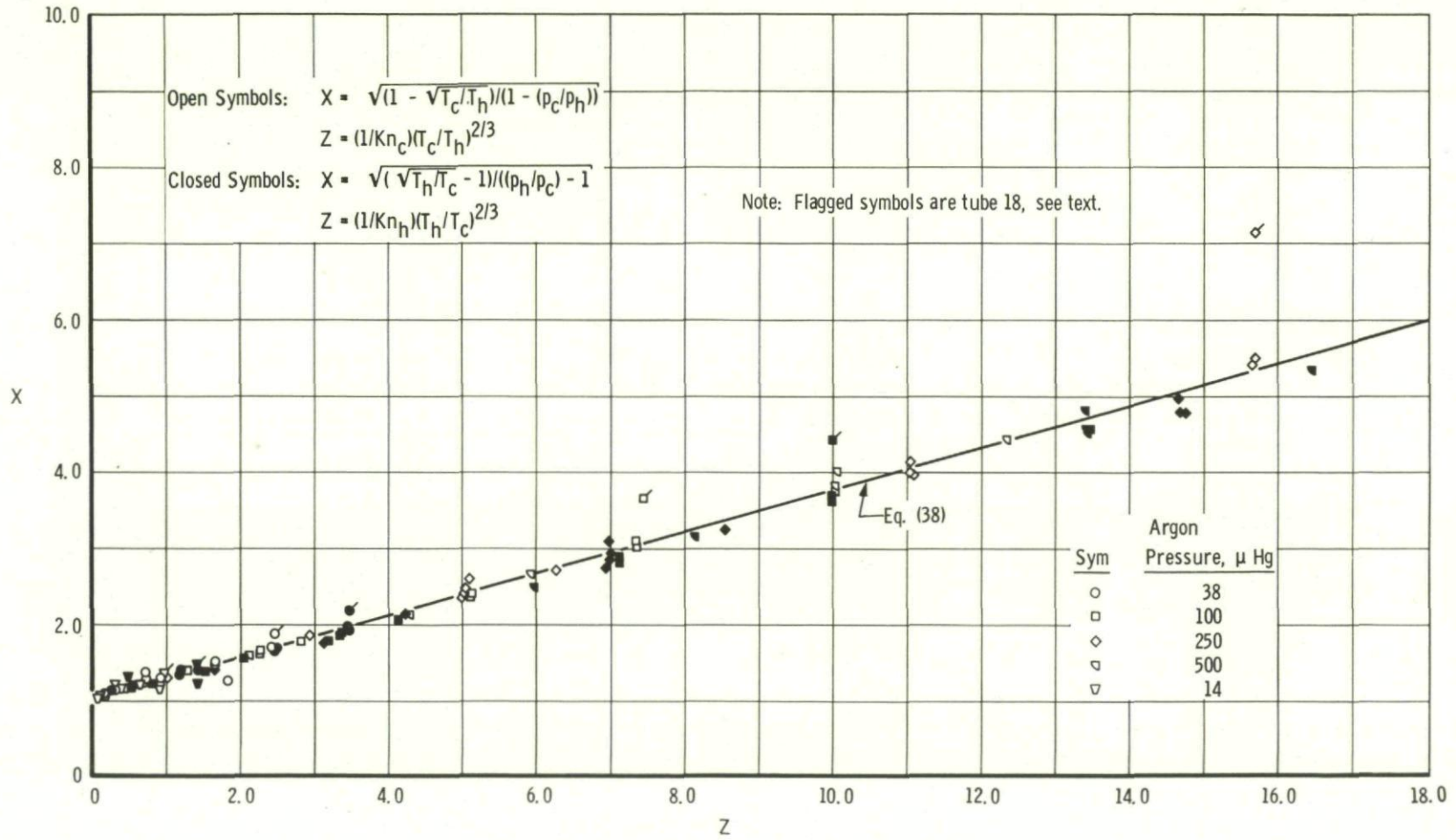


Fig. 9 Slip flow results for tubes using argon

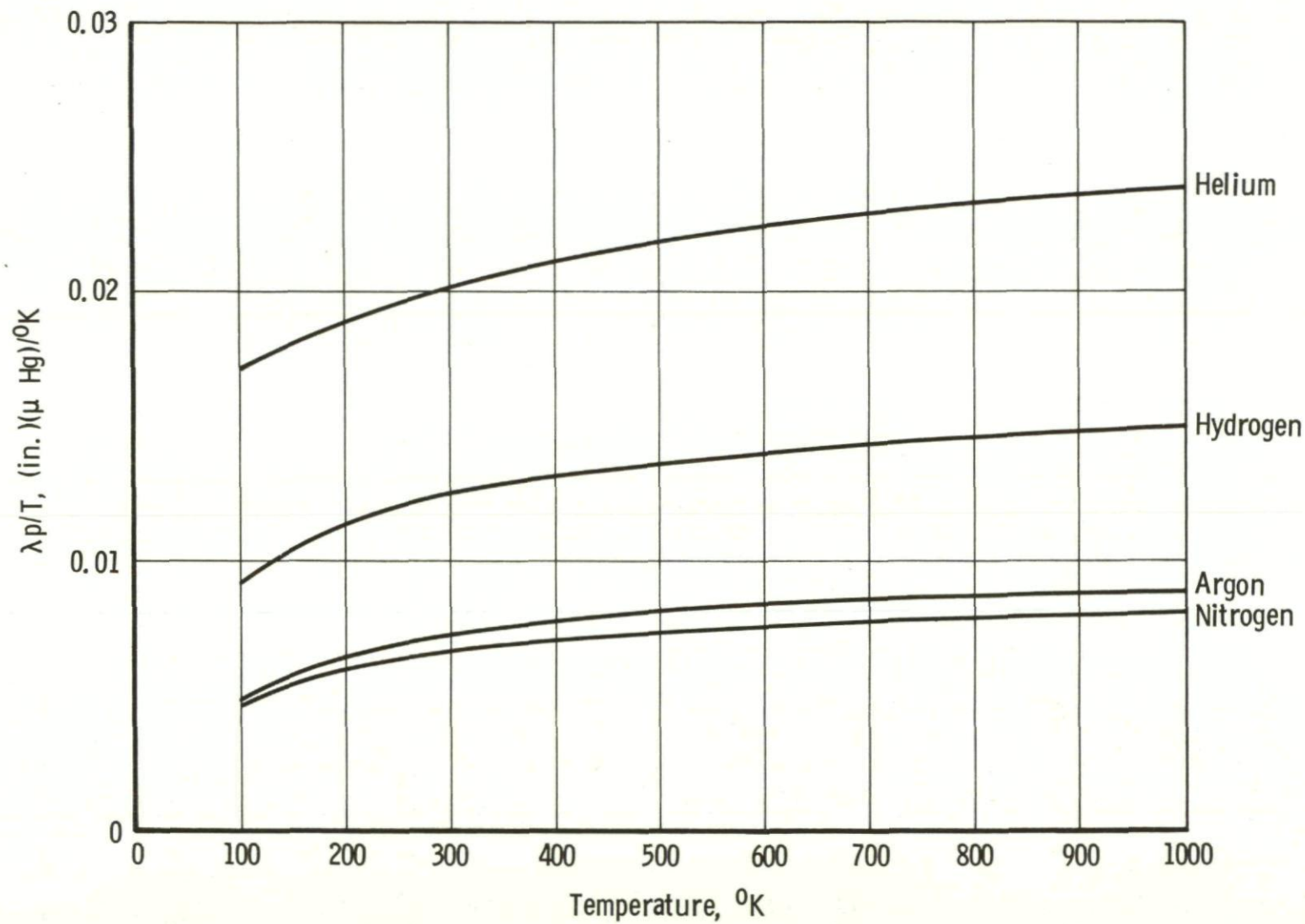


Fig. 10 Mean free path for gases tested

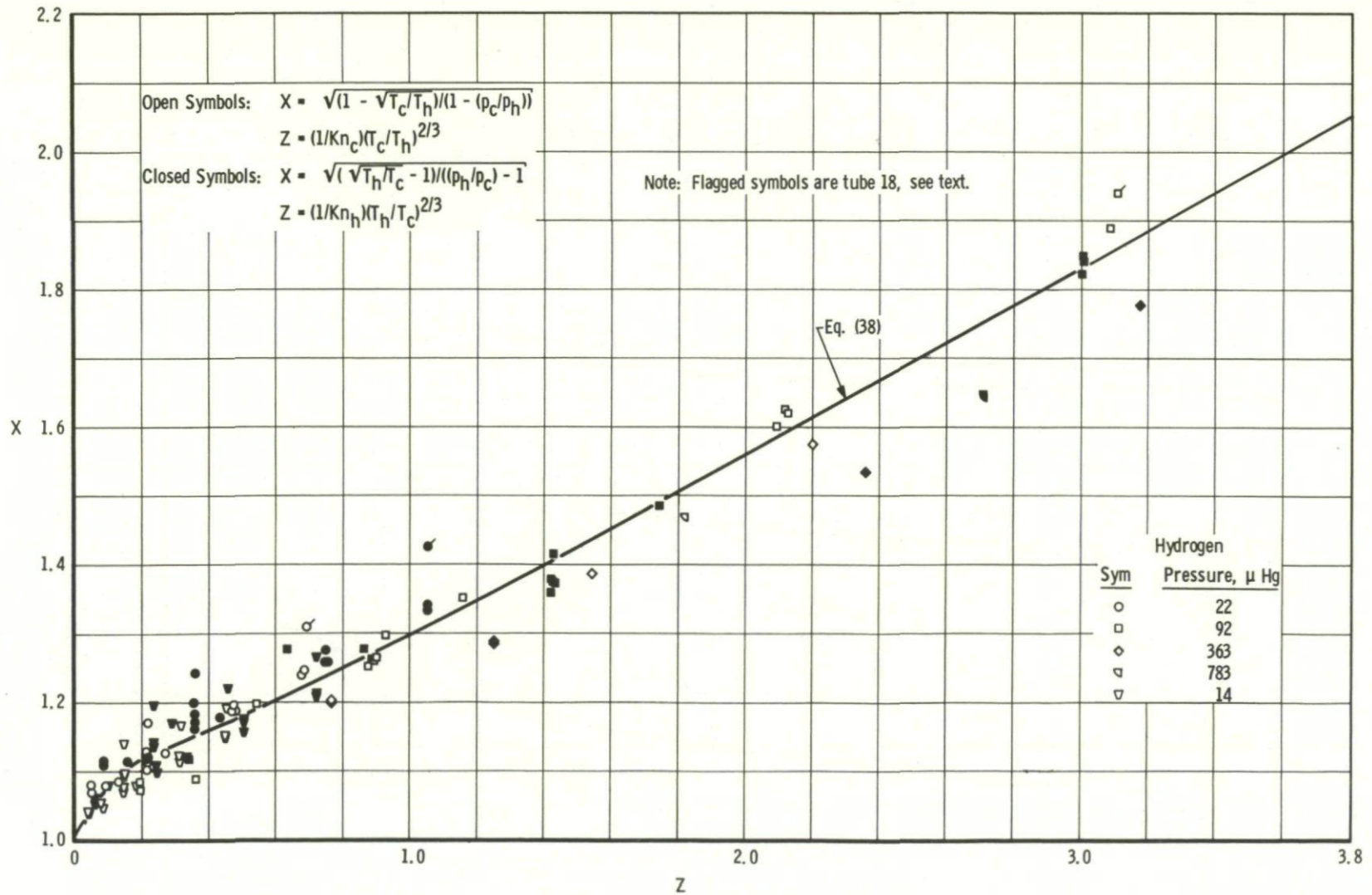


Fig. 11 Transitional results for tubes using hydrogen

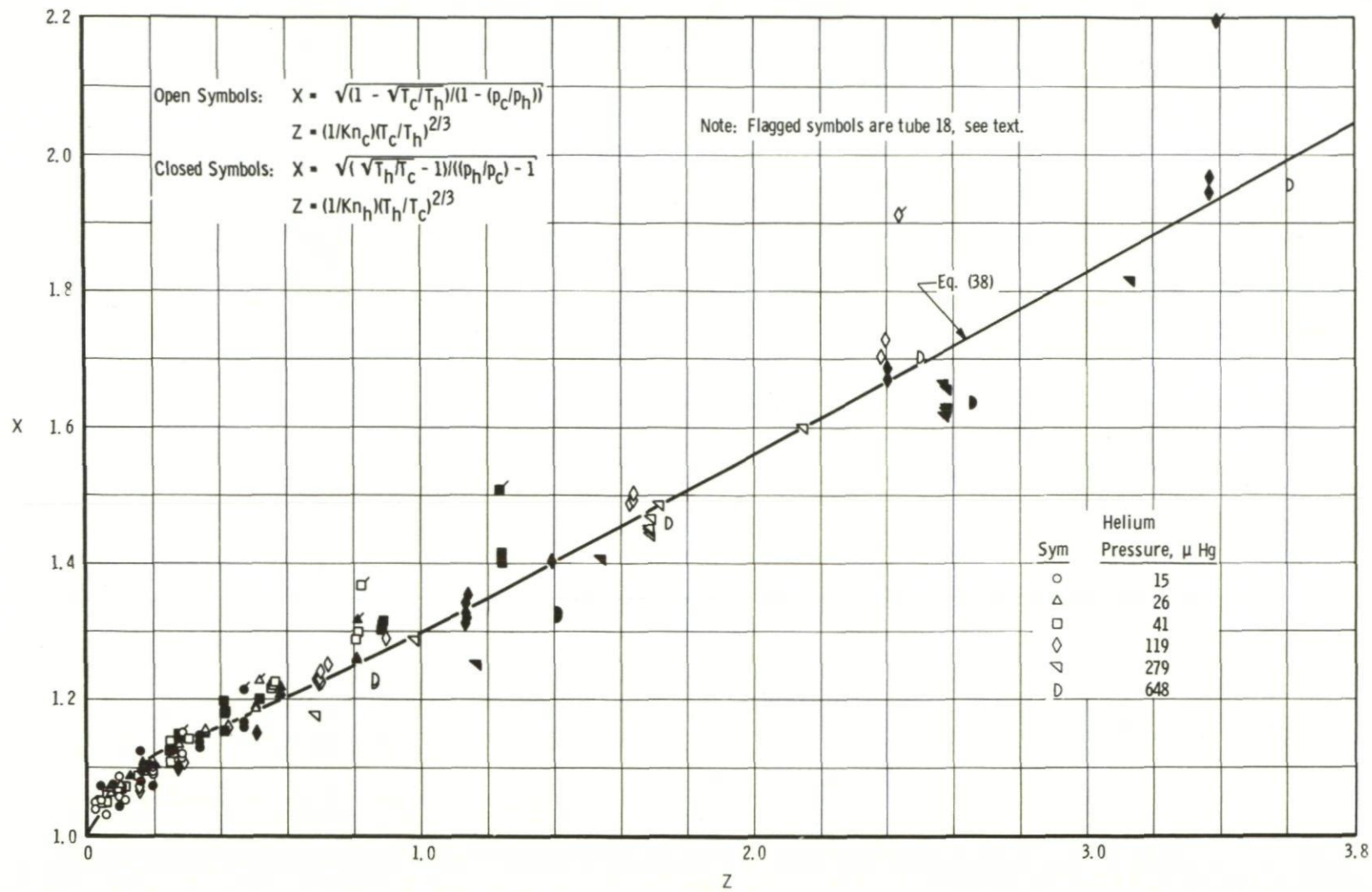


Fig. 12 Transitional results for tubes using helium

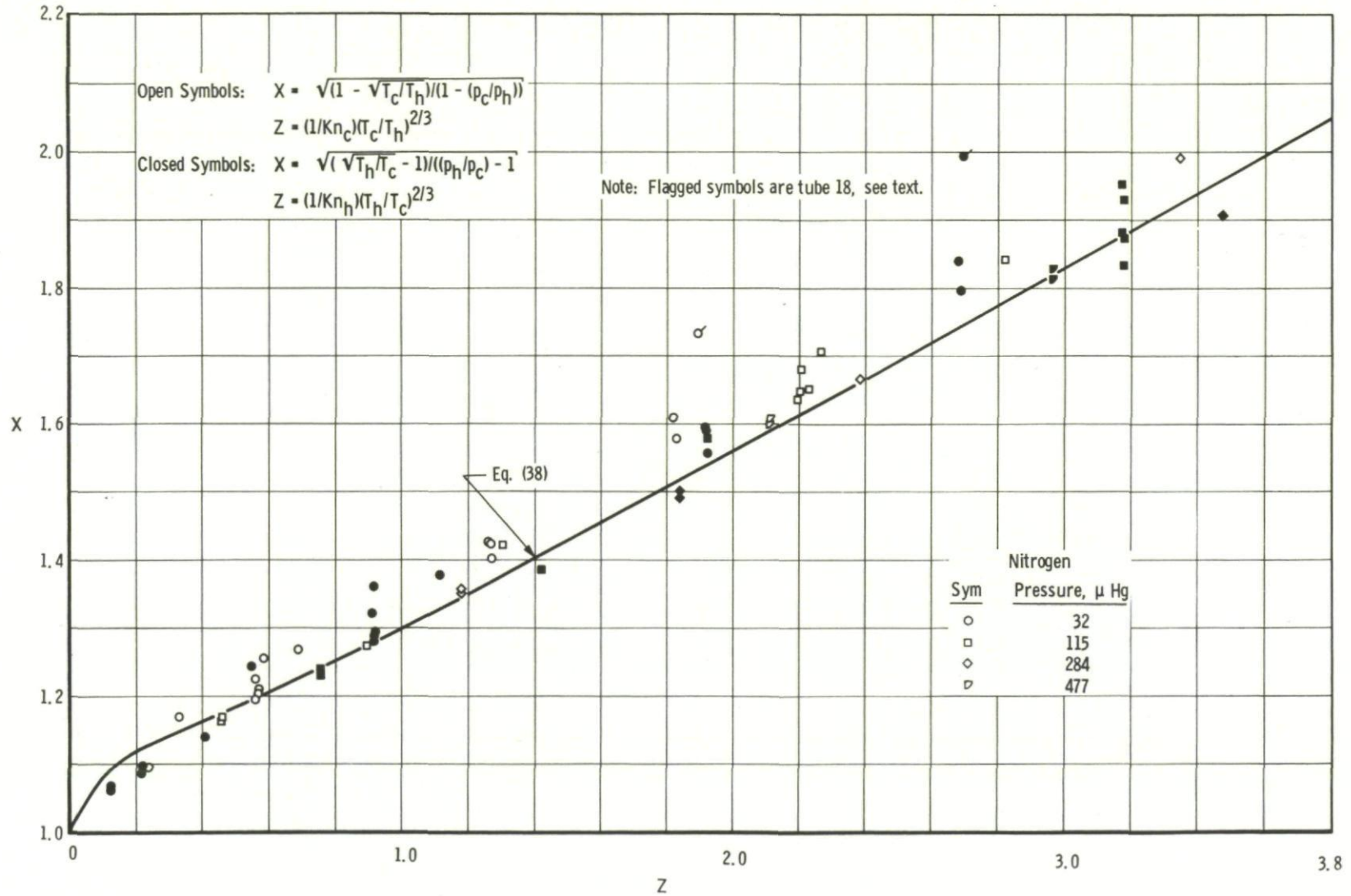


Fig. 13 Transitional results for tubes using nitrogen

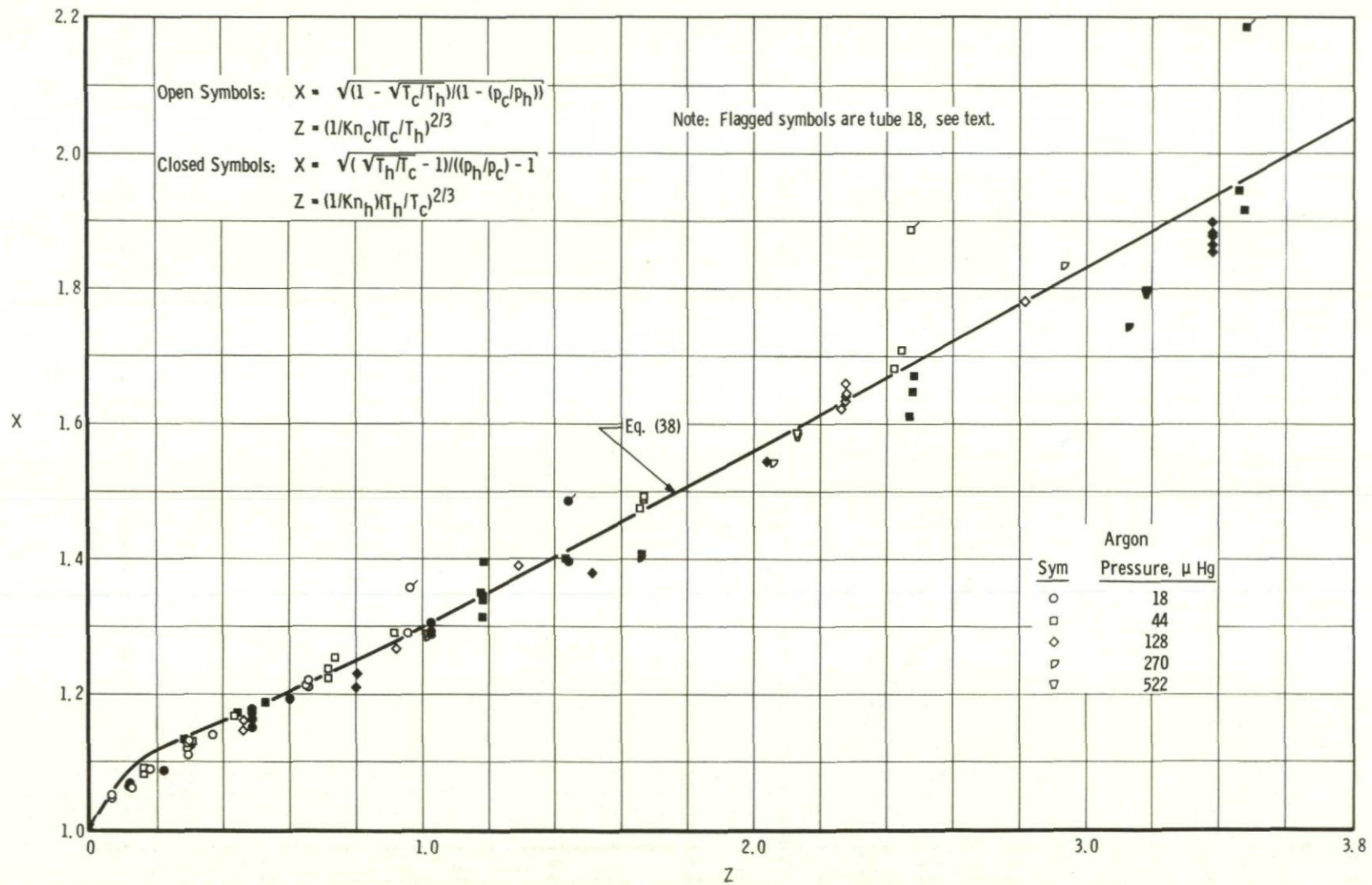


Fig. 14 Transitional results for tubes using argon

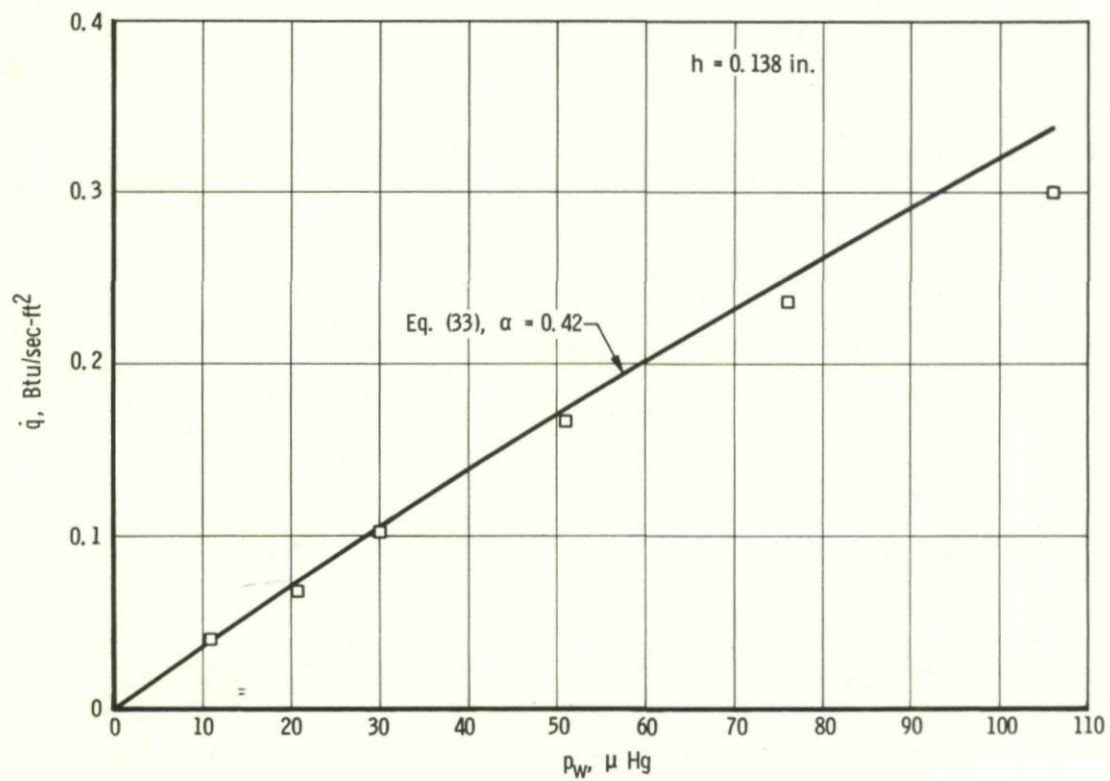
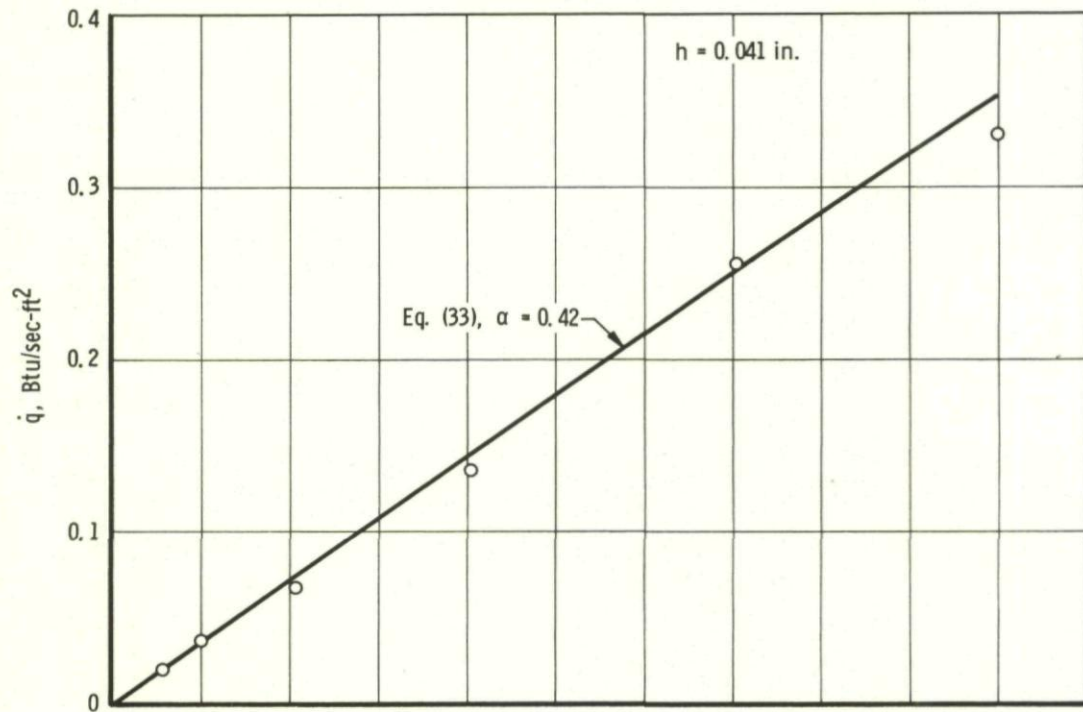


Fig. 15 Determination of α from measured \dot{q} for hydrogen

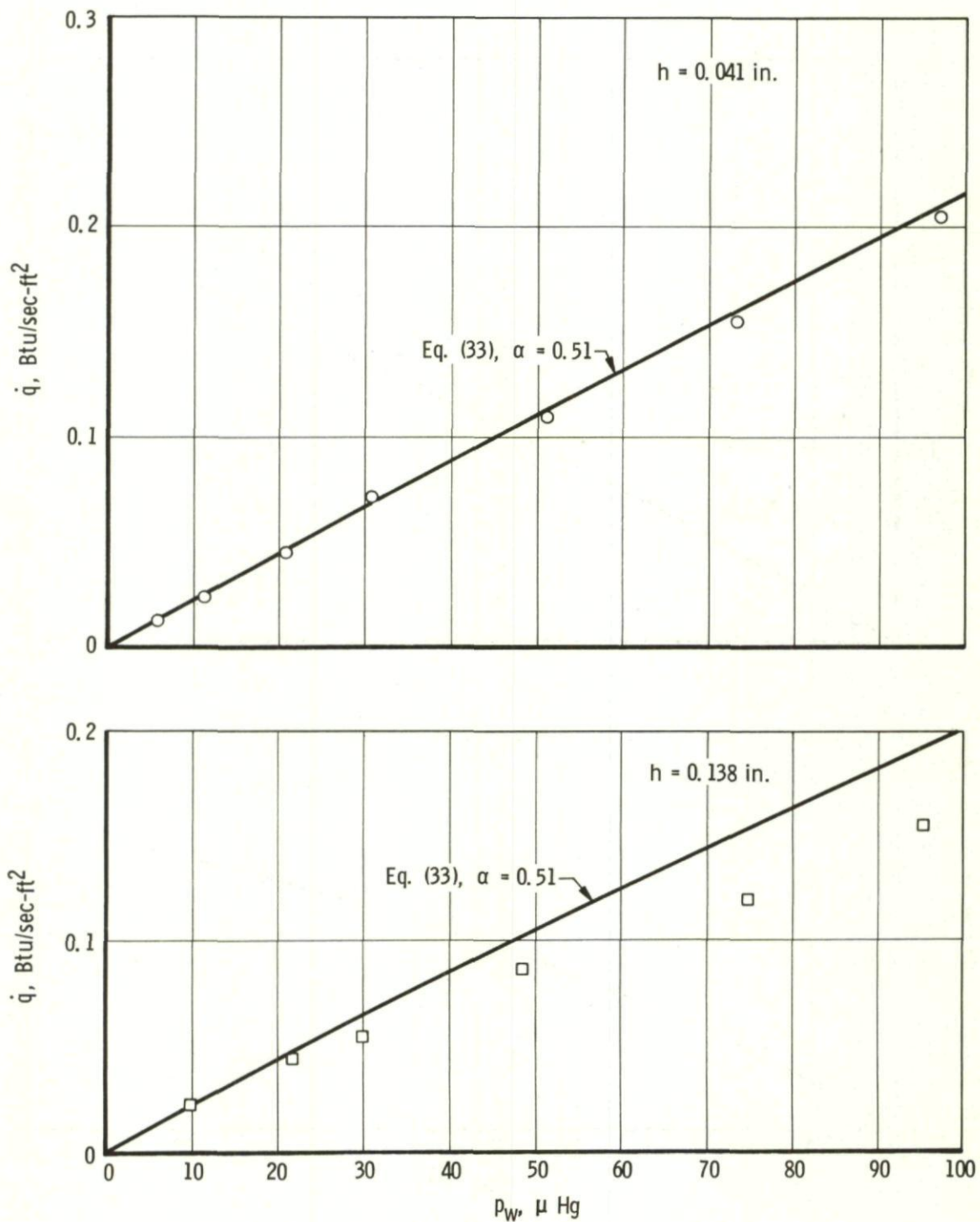


Fig. 16 Determination of α from measured \dot{q} for helium

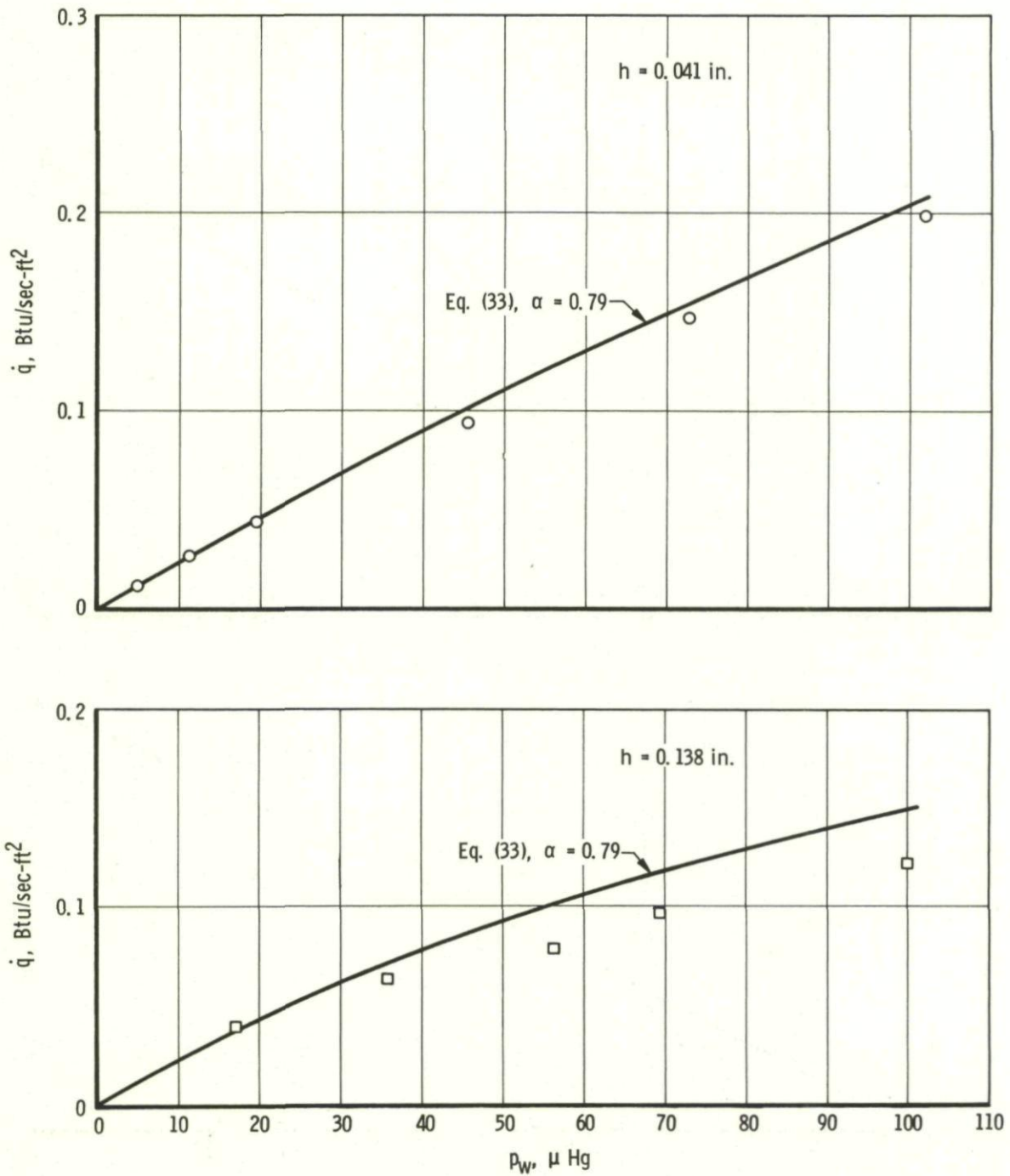


Fig. 17 Determination of α from measured \dot{q} for nitrogen

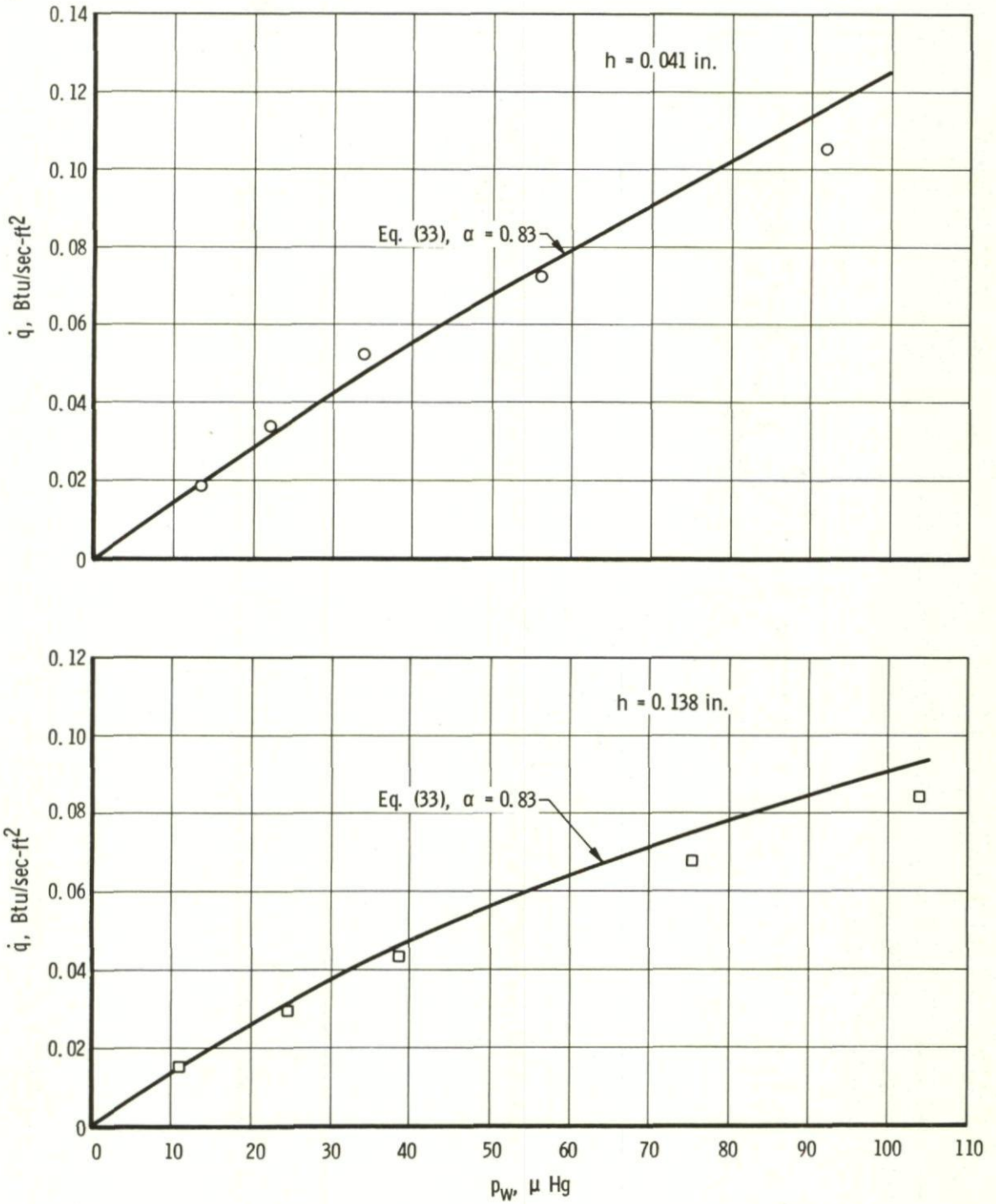


Fig. 18 Determination of α from measured \dot{q} for argon

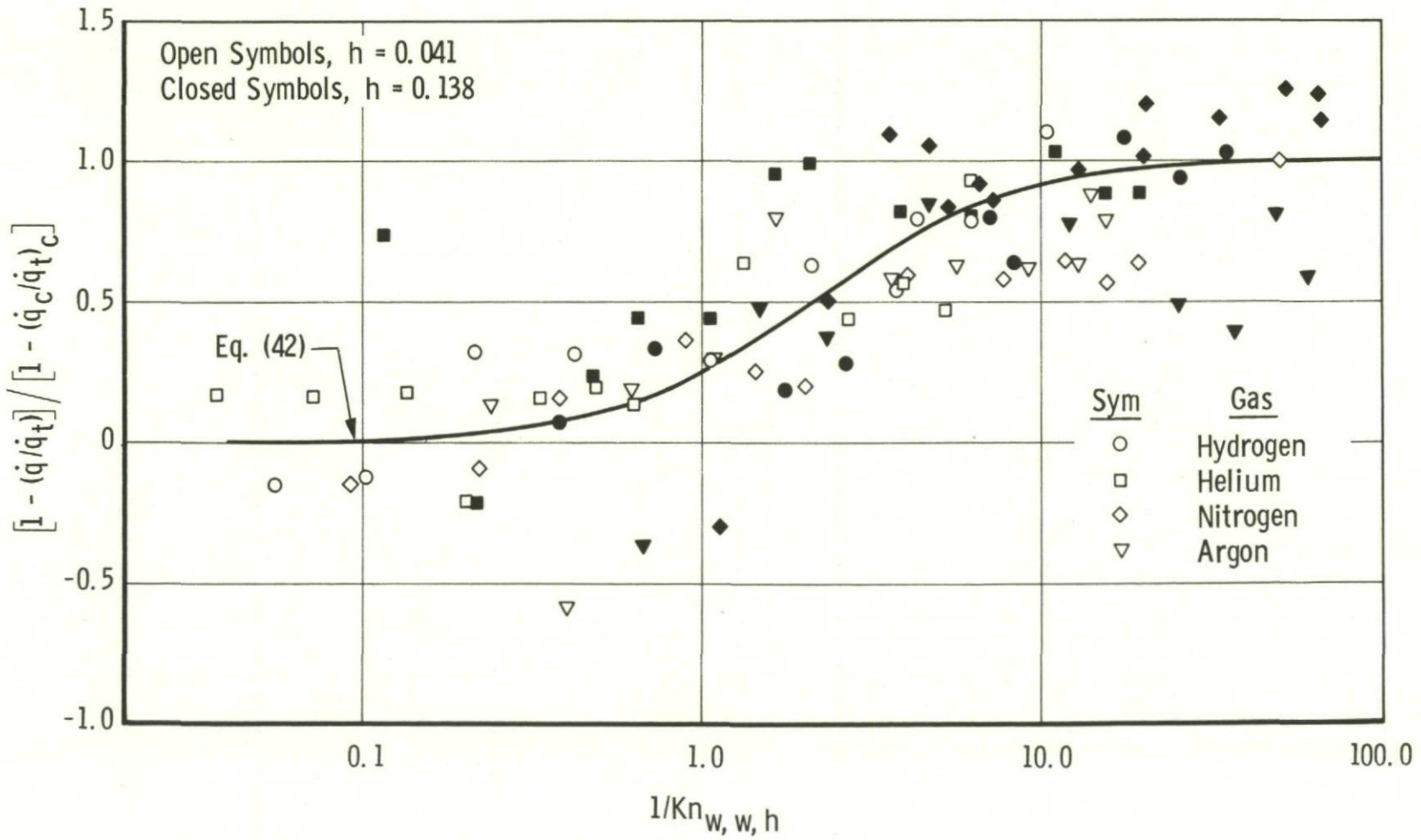


Fig. 19 Summary of heat-transfer results for all gases tested

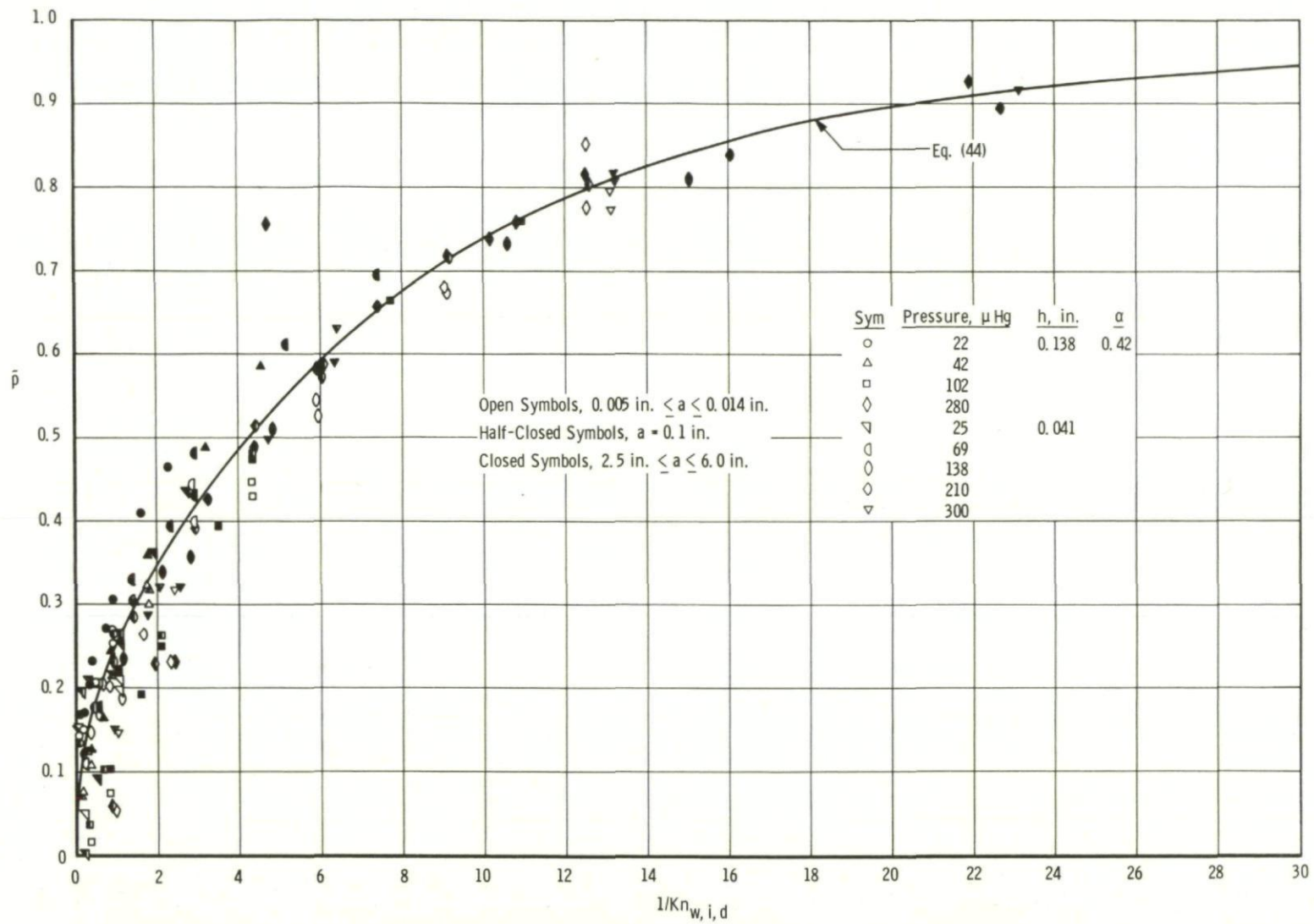


Fig. 20 Experimental results for circular orifices using hydrogen

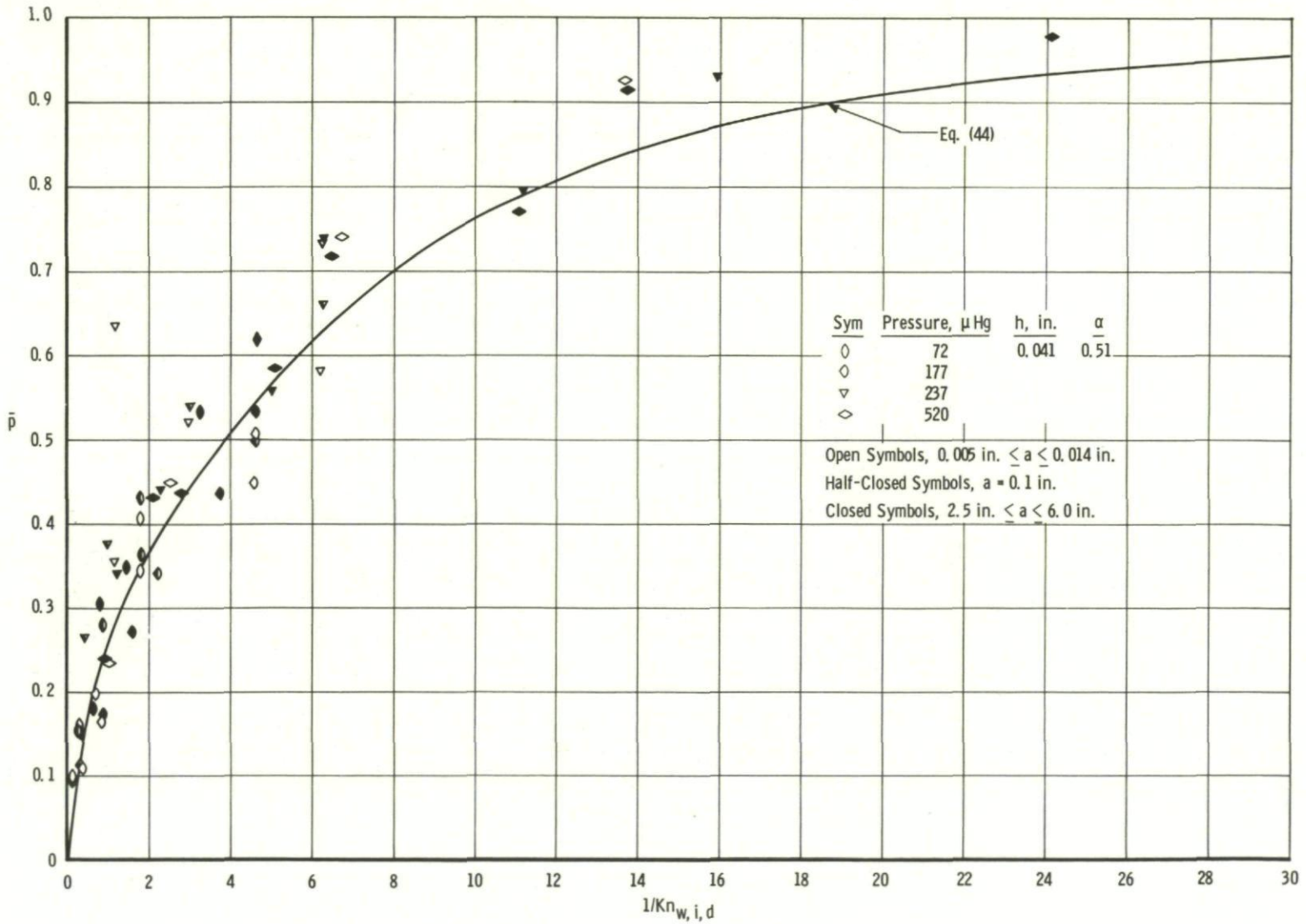


Fig. 21 Experimental results for circular orifices using helium

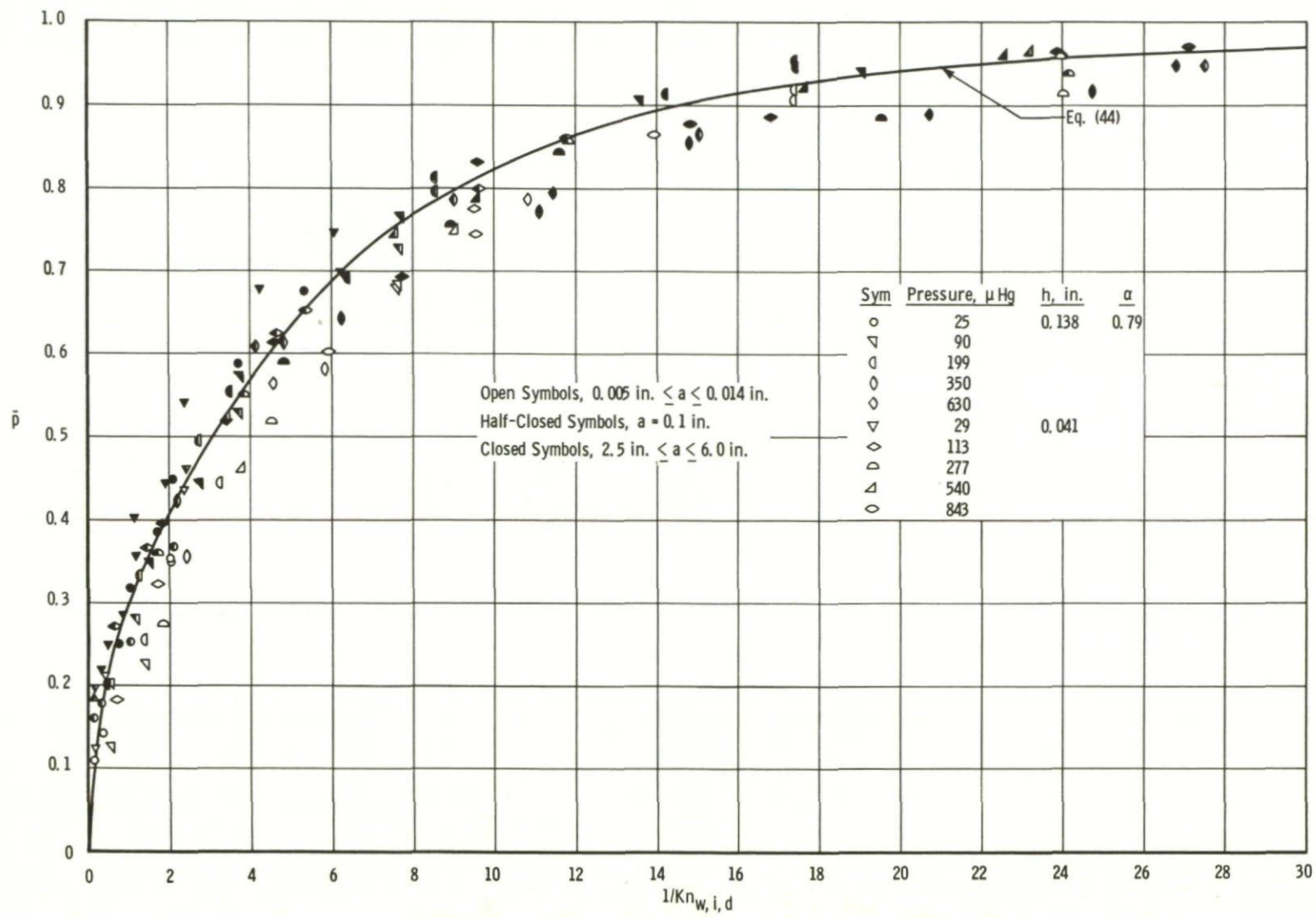


Fig. 22 Experimental results for circular orifices using nitrogen

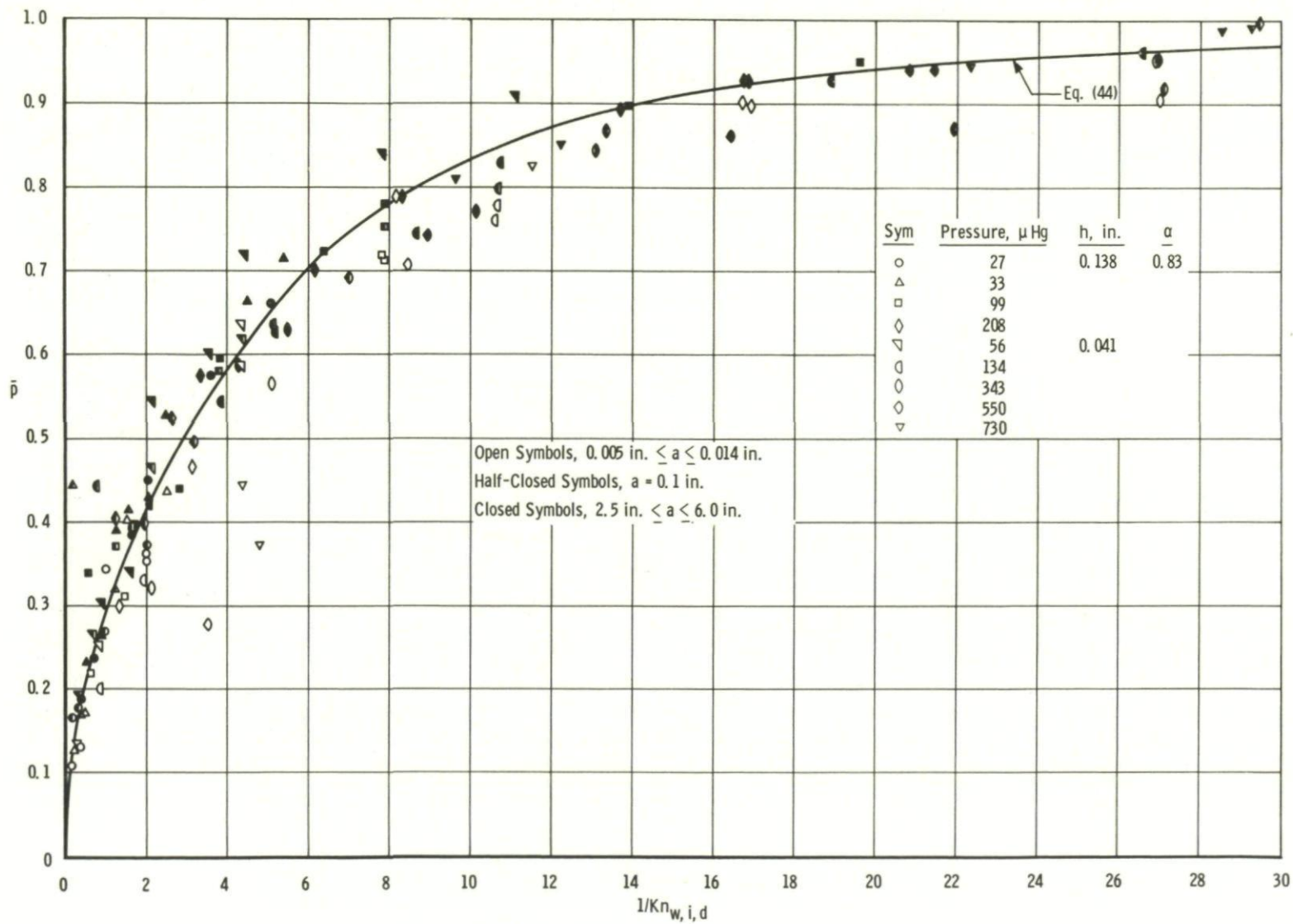


Fig. 23 Experimental results for circular orifices using argon

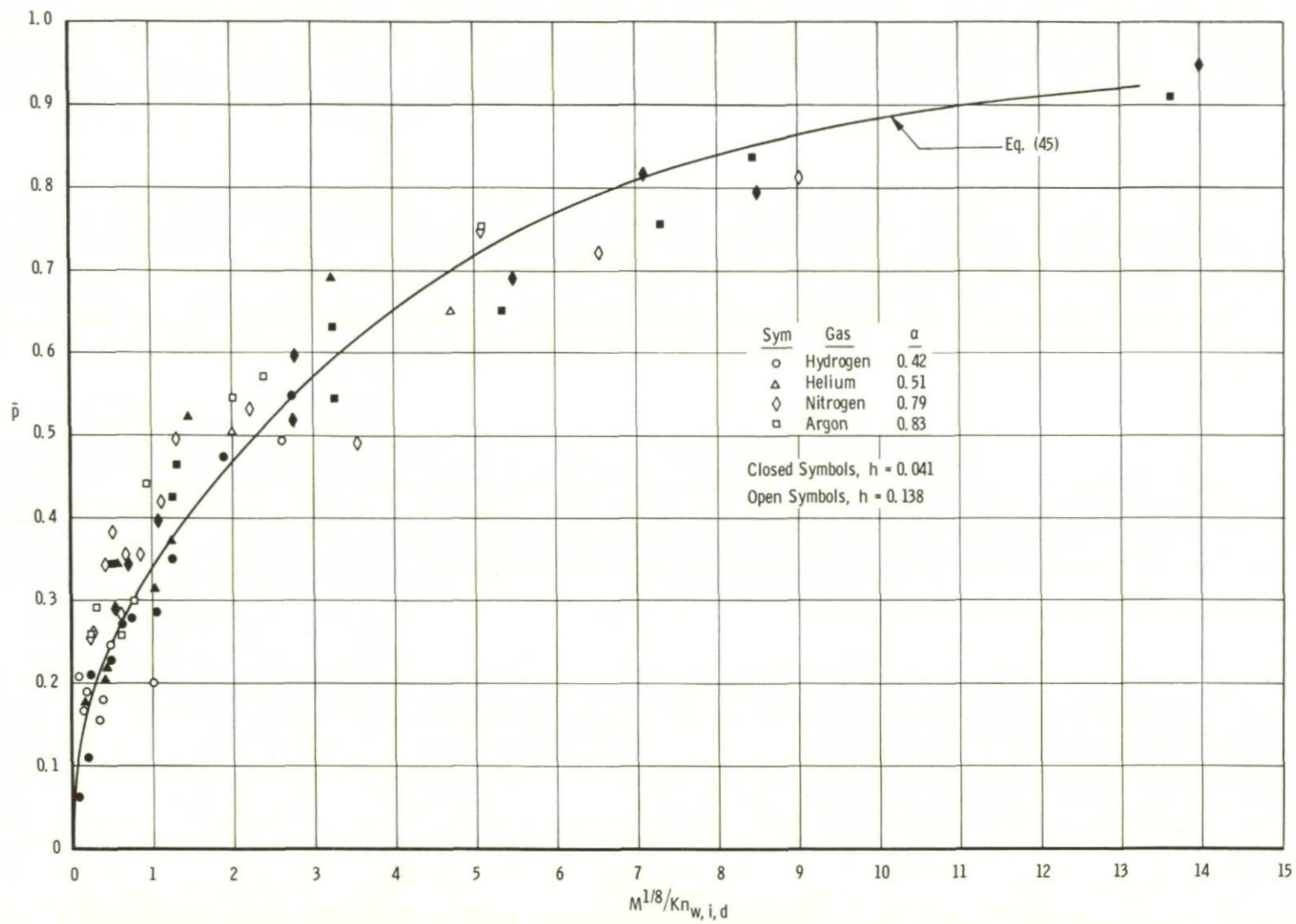


Fig. 24 Experimental results for annular orifices for all gases tested

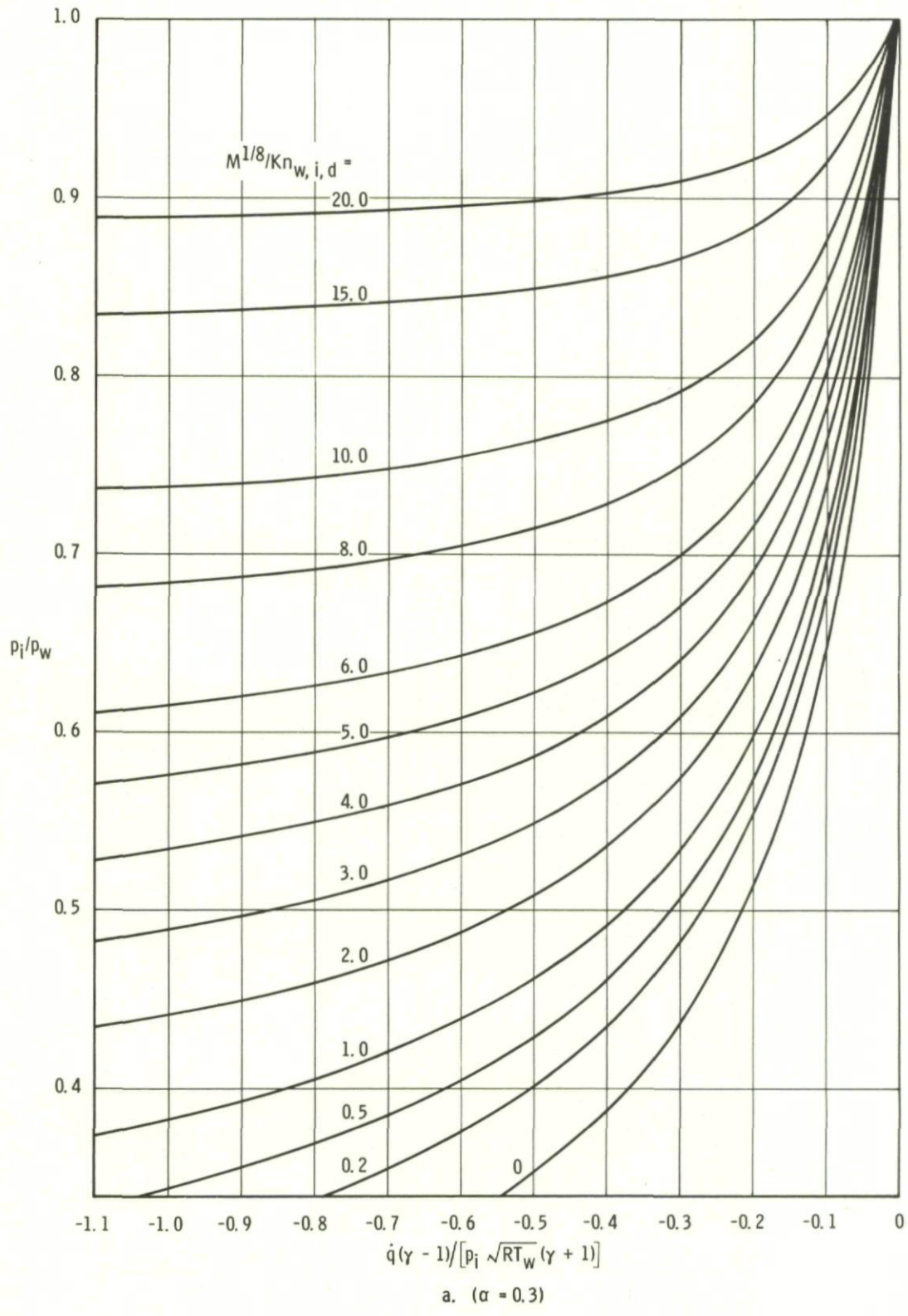


Fig. 25 Combined theoretical and experimental results for orifices

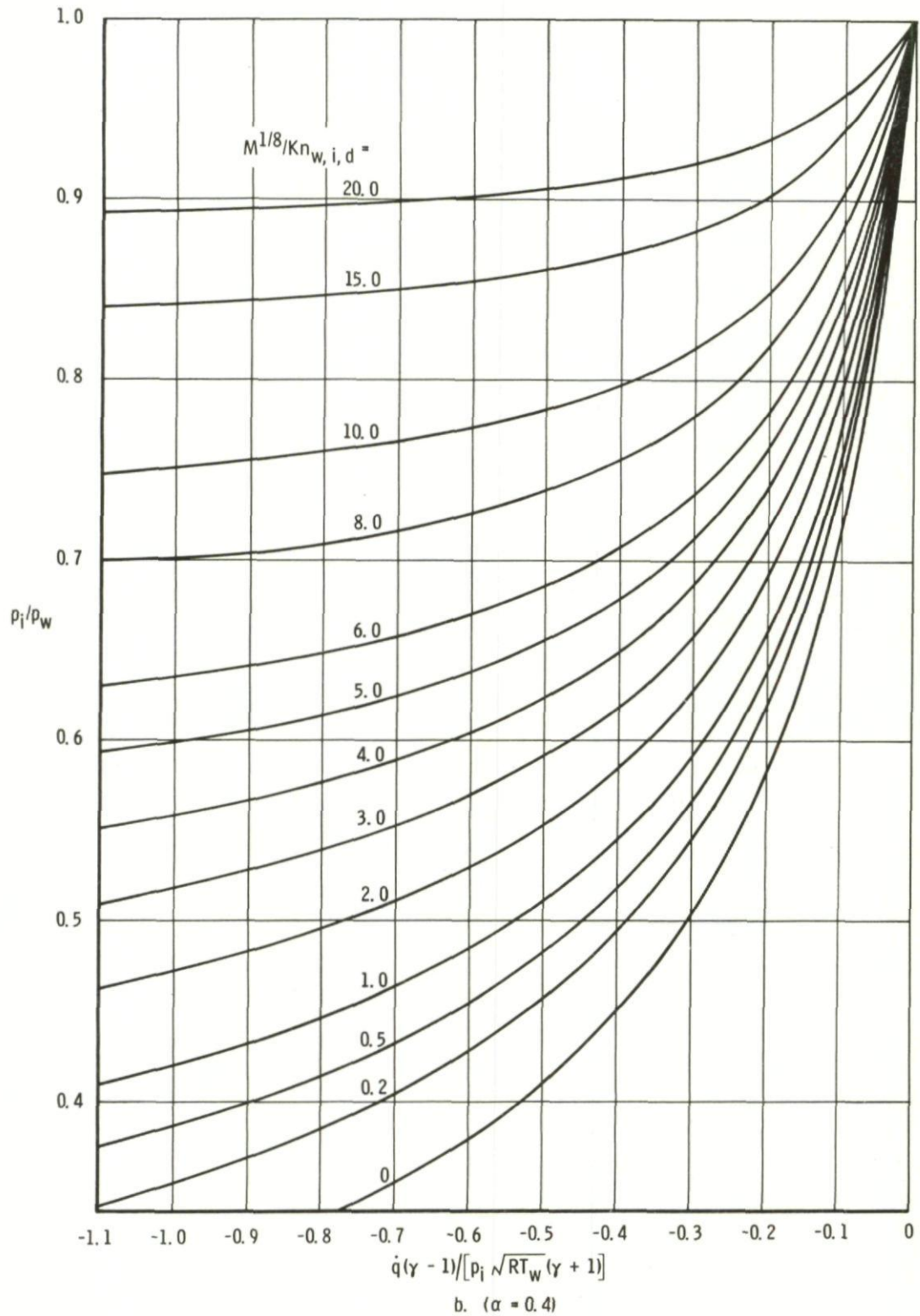


Fig. 25 Combined theoretical and experimental results for orifices (continued)

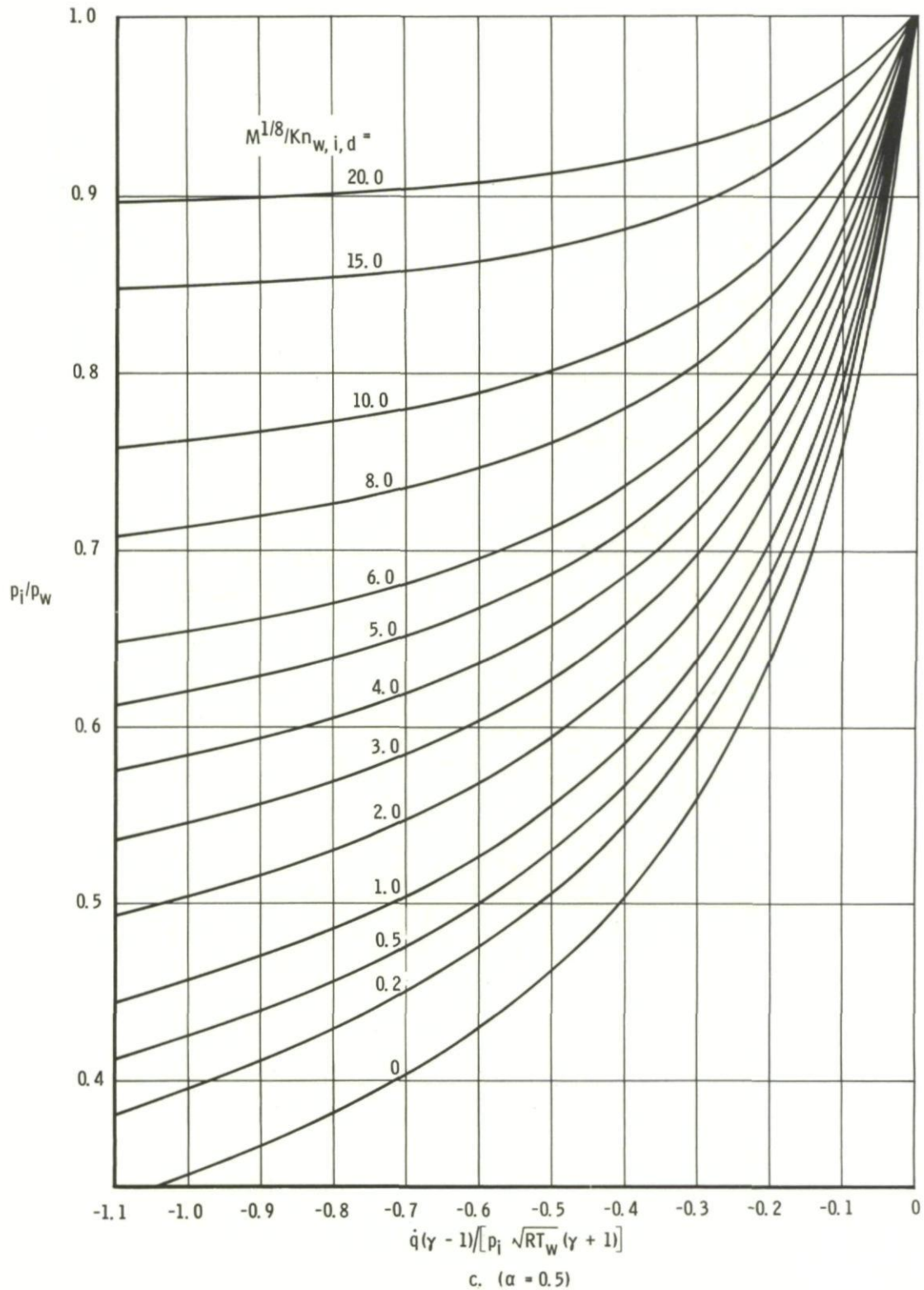


Fig. 25 Combined theoretical and experimental results for orifices (continued)

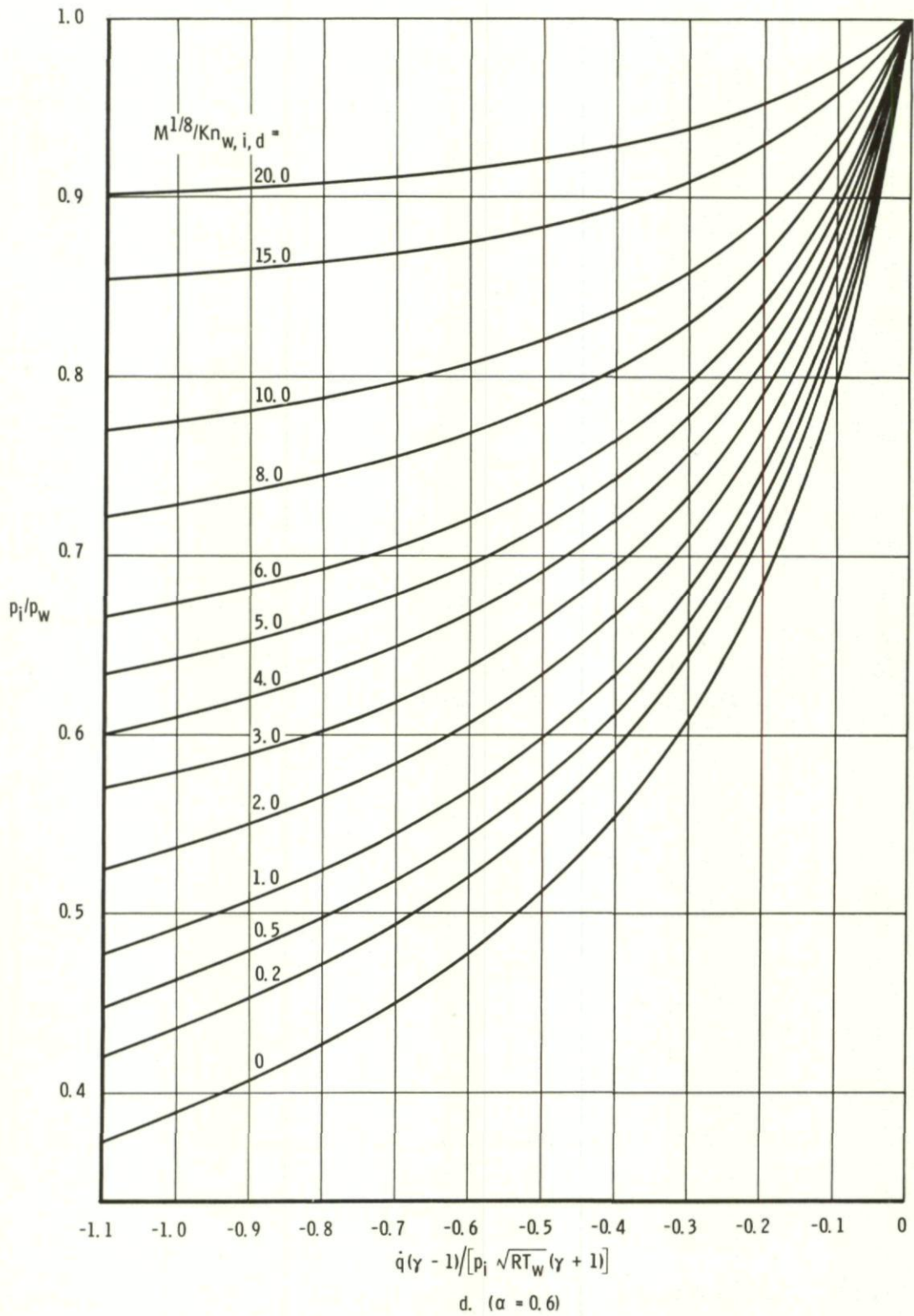


Fig. 25 Combined theoretical and experimental results for orifices (continued)

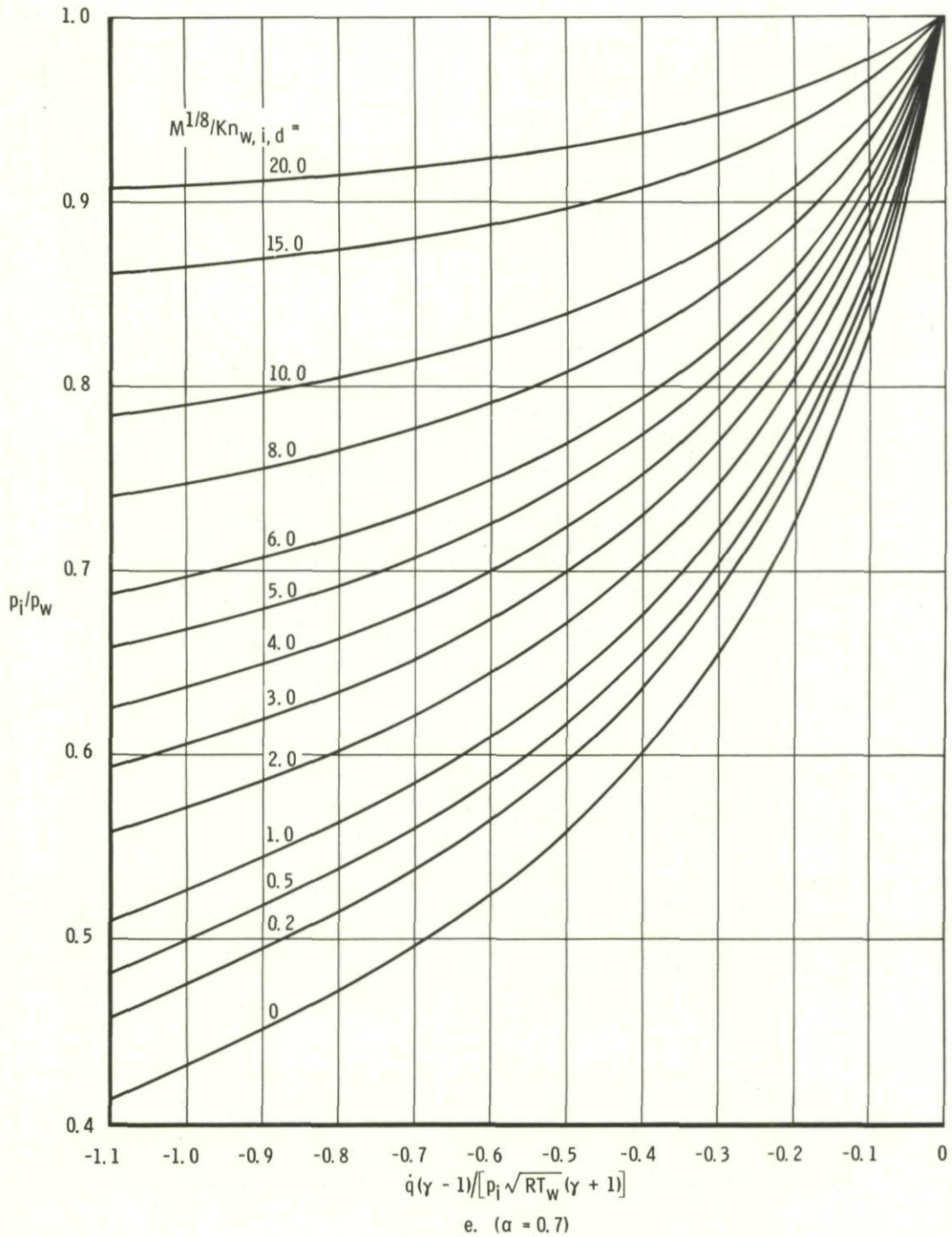


Fig. 25 Combined theoretical and experimental results for orifices (continued)

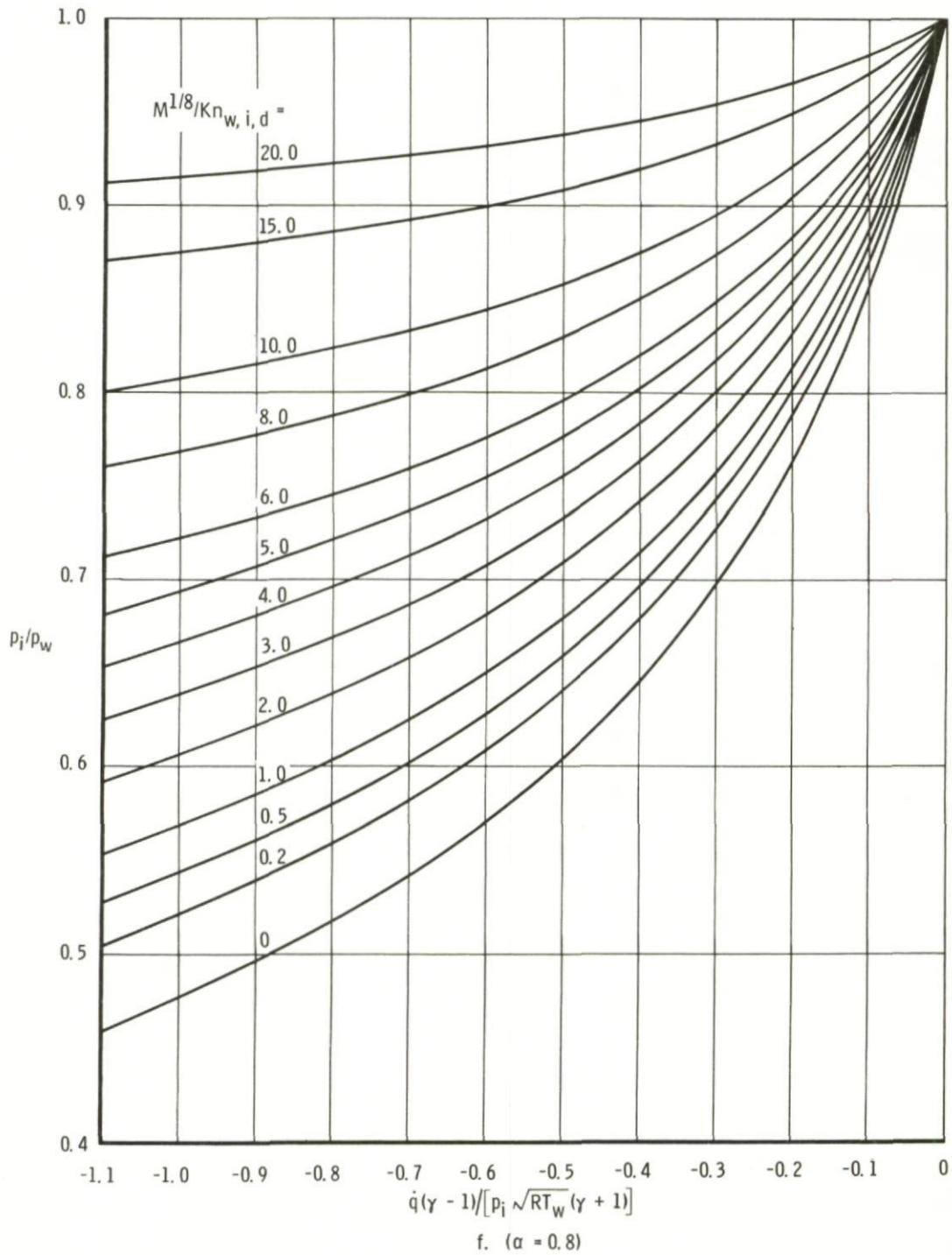


Fig. 25 Combined theoretical and experimental results for orifices (continued)

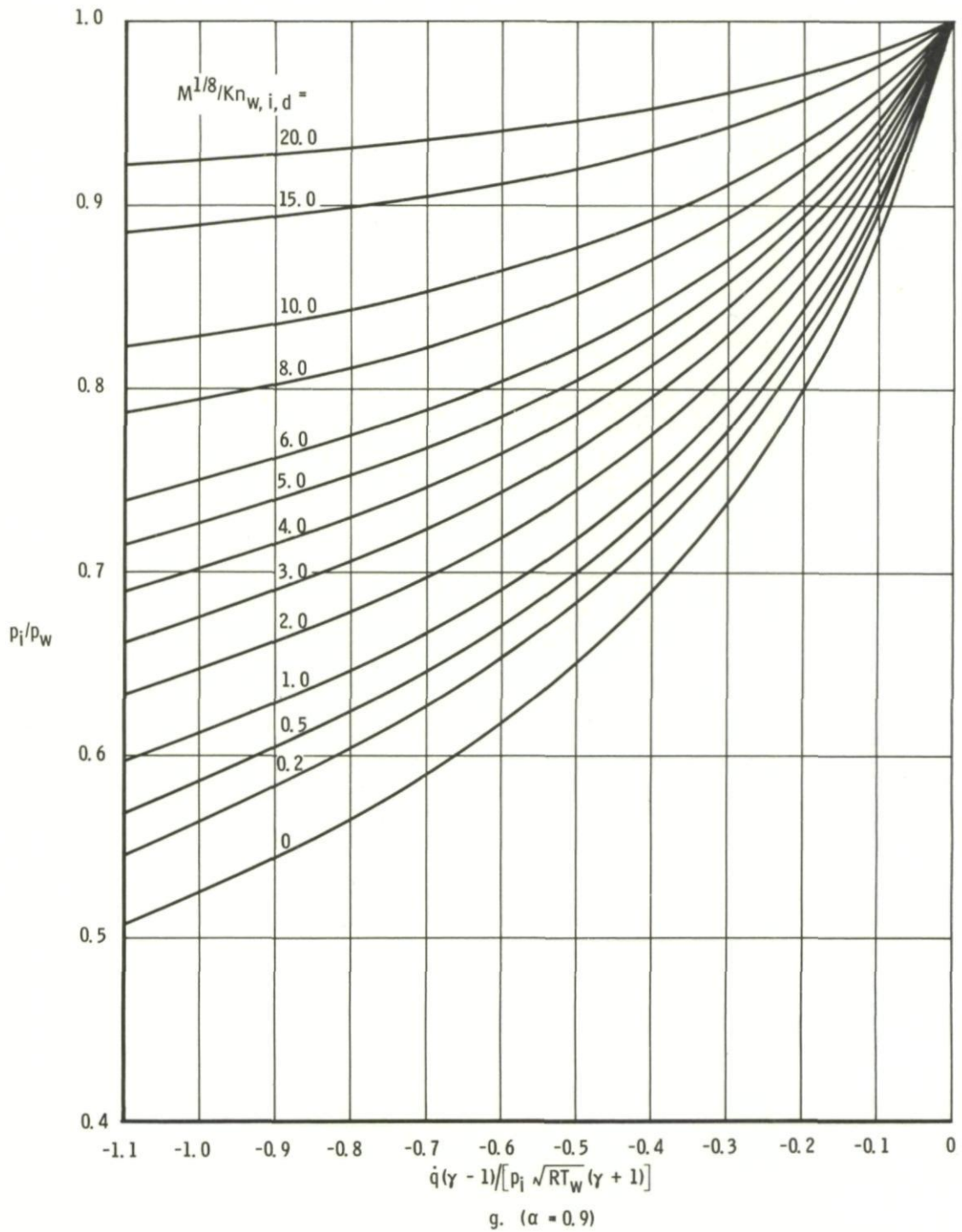


Fig. 25 Combined theoretical and experimental results for orifices (continued)

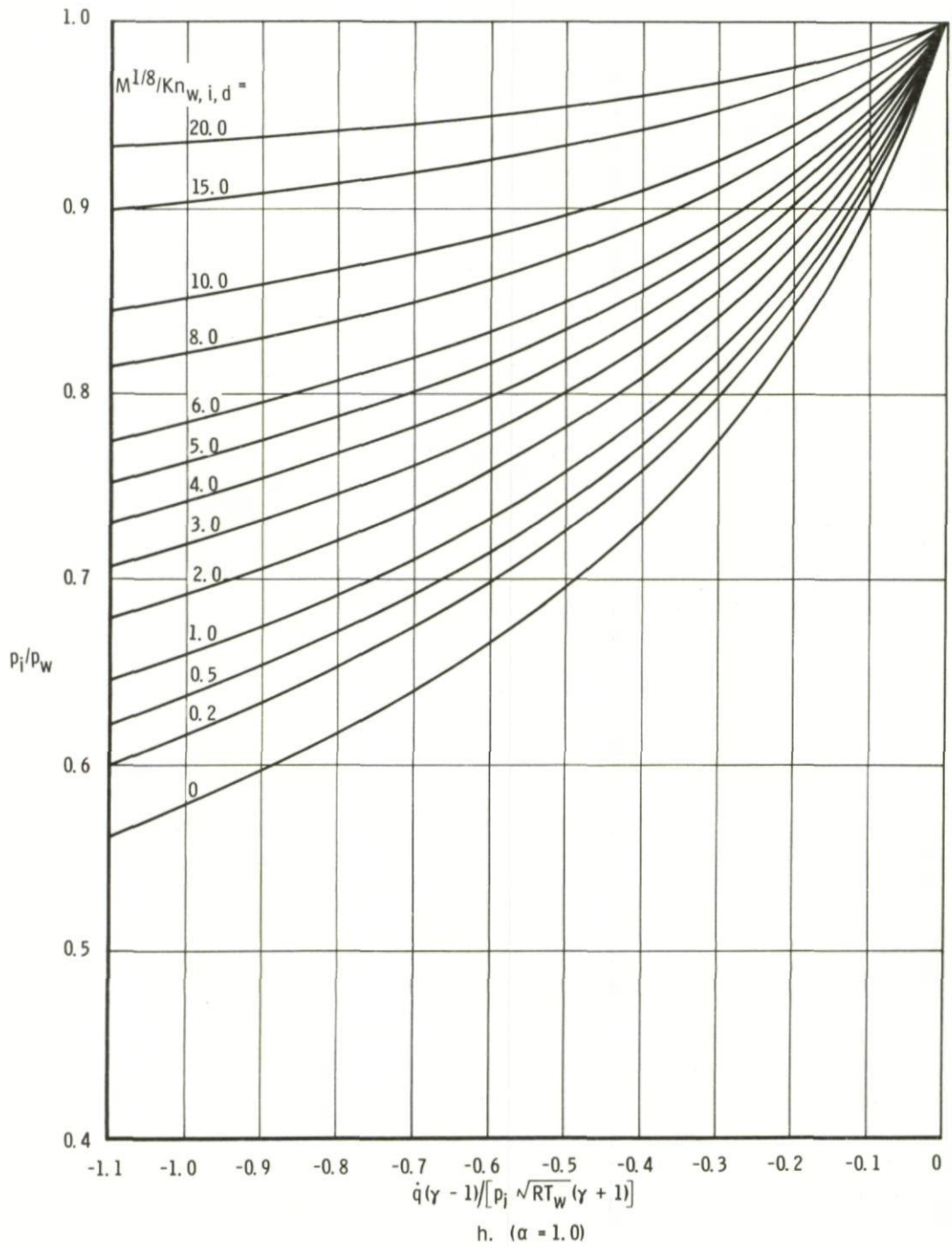


Fig. 25 Combined theoretical and experimental results for orifices (concluded)

DISTRIBUTION

Copies of AGARD publications may be obtained in the various countries at the addresses given below.

On peut se procurer des exemplaires des publications de l'AGARD aux adresses suivantes.

BELGIUM BELGIQUE	Centre National d'Etudes et de Recherches Aéronautiques 11, rue d'Egmont, Bruxelles
CANADA	Director of Scientific Information Service Defence Research Board Department of National Defence 'A' Building, Ottawa, Ontario
DENMARK DANEMARK	Danish Defence Research Board Østerbrogades Kaserne, Copenhagen, Ø
FRANCE	O.N.E.R.A. (Direction) 25, Av. de la Division Leclerc Châtillon-sous-Bagneux (Seine)
GERMANY ALLEMAGNE	Zentralstelle für Luftfahrtokumentation und Information 8 München 27 Maria-Theresia-Str.21 Attn: Dr. H.J. Rautenberg
GREECE GRECE	Greek National Defence General Staff B. JSG, Athens
ICELAND ISLANDE	Director of Aviation c/o Flugrad, Reykjavik
ITALY ITALIE	Ufficio del Delegato Nazionale all'AGARD Ministero Difesa - Aeronautica Roma
LUXEMBURG LUXEMBOURG	Obtainable through Belgium
NETHERLANDS PAYS BAS	Netherlands Delegation to AGARD Kluyverweg 1, Delft

NORWAY
NORVEGE

Norwegian Defence
Research Establishment
Kjeller per Lilleström
Attn: Mr. O. Blichner

PORTUGAL

Delegado Nacional do 'AGARD'
Direcção do Serviço de Material
da Forca Aerea
Rua da Escola Politecnica, 42
Lisboa

TURKEY
TURQUIE

Ministry of National Defence
Ankara
Attn: AGARD National Delegate

UNITED KINGDOM
ROYAUME UNI

Ministry of Aviation
T.I.L. 1,
Block A,
Station Square House,
St. Mary Cray,
Orpington, Kent

UNITED STATES
ETATS UNIS

National Aeronautics and Space Administration
(NASA)
Washington, D.C. 20546





<p>AGARDograph 119 North Atlantic Treaty Organization, Advisory Group for Aerospace Research and Development THERMO-MOLECULAR PRESSURE EFFECTS IN TUBES AND AT ORIFICES Max Kinslow and George D. Arney, Jr August 1967 57 pages incl. 22 refs, 25 figs.</p> <p>An investigation of the errors arising from thermal nonequilibrium in systems measuring gas pressures is presented. The errors are attributed to a phenomenon referred to as thermo-molecular pressure. This effect is investigated both theoretically and experimentally at sensing orifices and in tubes. A thorough review of the literature is given and a</p> <p style="text-align: right;">P. T. O.</p>	<p style="text-align: center;">532.522:532.575.6</p>	<p>AGARDograph 119 North Atlantic Treaty Organization, Advisory Group for Aerospace Research and Development THERMO-MOLECULAR PRESSURE EFFECTS IN TUBES AND AT ORIFICES Max Kinslow and George D. Arney, Jr August 1967 57 pages incl. 22 refs, 25 figs.</p> <p>An investigation of the errors arising from thermal nonequilibrium in systems measuring gas pressures is presented. The errors are attributed to a phenomenon referred to as thermo-molecular pressure. This effect is investigated both theoretically and experimentally at sensing orifices and in tubes. A thorough review of the literature is given and a</p> <p style="text-align: right;">P. T. O.</p>	<p style="text-align: center;">532.522:532.575.6</p>
<p>AGARDograph 119 North Atlantic Treaty Organization, Advisory Group for Aerospace Research and Development THERMO-MOLECULAR PRESSURE EFFECTS IN TUBES AND AT ORIFICES Max Kinslow and George D. Arney, Jr August 1967 57 pages incl. 22 refs, 25 figs.</p> <p>An investigation of the errors arising from thermal nonequilibrium in systems measuring gas pressures is presented. The errors are attributed to a phenomenon referred to as thermo-molecular pressure. This effect is investigated both theoretically and experimentally at sensing orifices and in tubes. A thorough review of the literature is given and a</p> <p style="text-align: right;">P. T. O.</p>	<p style="text-align: center;">532.522:532.575.6</p>	<p>AGARDograph 119 North Atlantic Treaty Organization, Advisory Group for Aerospace Research and Development THERMO-MOLECULAR PRESSURE EFFECTS IN TUBES AND AT ORIFICES Max Kinslow and George D. Arney, Jr August 1967 57 pages incl. 22 refs, 25 figs.</p> <p>An investigation of the errors arising from thermal nonequilibrium in systems measuring gas pressures is presented. The errors are attributed to a phenomenon referred to as thermo-molecular pressure. This effect is investigated both theoretically and experimentally at sensing orifices and in tubes. A thorough review of the literature is given and a</p> <p style="text-align: right;">P. T. O.</p>	<p style="text-align: center;">532.522:532.575.6</p>

theory is developed for the error introduced in the limiting case of a very small sensing orifice with heat flux to the orifice surface. The theory takes into account the effect of arbitrary thermal accommodation coefficient at the orifice surface. Experimental data are presented separately for thermo-molecular pressures in tubes and at orifices. In addition, results of heat-transfer measurements in the transitional flow regime between flat plates are presented as a basis for correlating the orifice data. Finally, methods are given, with examples, for the correction of thermo-molecular effects both at orifices and in circular tubes.

This is one of a series of publications by the NATO-AGARD Fluid Dynamics Panel. Professor Wilbur C. Nelson of The University of Michigan is the Editor

theory is developed for the error introduced in the limiting case of a very small sensing orifice with heat flux to the orifice surface. The theory takes into account the effect of arbitrary thermal accommodation coefficient at the orifice surface. Experimental data are presented separately for thermo-molecular pressures in tubes and at orifices. In addition, results of heat-transfer measurements in the transitional flow regime between flat plates are presented as a basis for correlating the orifice data. Finally, methods are given, with examples, for the correction of thermo-molecular effects both at orifices and in circular tubes.

This is one of a series of publications by the NATO-AGARD Fluid Dynamics Panel. Professor Wilbur C. Nelson of The University of Michigan is the Editor

theory is developed for the error introduced in the limiting case of a very small sensing orifice with heat flux to the orifice surface. The theory takes into account the effect of arbitrary thermal accommodation coefficient at the orifice surface. Experimental data are presented separately for thermo-molecular pressures in tubes and at orifices. In addition, results of heat-transfer measurements in the transitional flow regime between flat plates are presented as a basis for correlating the orifice data. Finally, methods are given, with examples, for the correction of thermo-molecular effects both at orifices and in circular tubes..

This is one of a series of publications by the NATO-AGARD Fluid Dynamics Panel. Professor Wilbur C. Nelson of The University of Michigan is the Editor

theory is developed for the error introduced in the limiting case of a very small sensing orifice with heat flux to the orifice surface. The theory takes into account the effect of arbitrary thermal accommodation coefficient at the orifice surface. Experimental data are presented separately for thermo-molecular pressures in tubes and at orifices. In addition, results of heat-transfer measurements in the transitional flow regime between flat plates are presented as a basis for correlating the orifice data. Finally, methods are given, with examples, for the correction of thermo-molecular effects both at orifices and in circular tubes.

This is one of a series of publications by the NATO-AGARD Fluid Dynamics Panel. Professor Wilbur C. Nelson of The University of Michigan is the Editor

<p>AGARDograph 119 North Atlantic Treaty Organization, Advisory Group for Aerospace Research and Development THERMO-MOLECULAR PRESSURE EFFECTS IN TUBES AND AT ORIFICES Max Kinslow and George D. Arney, Jr August 1967 57 pages incl. 22 refs, 25 figs.</p> <p>An investigation of the errors arising from thermal nonequilibrium in systems measuring gas pressures is presented. The errors are attributed to a phenomenon referred to as thermo-molecular pressure. This effect is investigated both theoretically and experimentally at sensing orifices and in tubes. A thorough review of the literature is given and a</p> <p style="text-align: right;">P. T. O.</p>	<p style="text-align: center;">532.522:532.575.6</p>	<p>AGARDograph 119 North Atlantic Treaty Organization, Advisory Group for Aerospace Research and Development THERMO-MOLECULAR PRESSURE EFFECTS IN TUBES AND AT ORIFICES Max Kinslow and George D. Arney, Jr August 1967 57 pages incl. 22 refs, 25 figs.</p> <p>An investigation of the errors arising from thermal nonequilibrium in systems measuring gas pressures is presented. The errors are attributed to a phenomenon referred to as thermo-molecular pressure. This effect is investigated both theoretically and experimentally at sensing orifices and in tubes. A thorough review of the literature is given and a</p> <p style="text-align: right;">P. T. O.</p>	<p style="text-align: center;">532.522:532.575.6</p>
<p>AGARDograph 119 North Atlantic Treaty Organization, Advisory Group for Aerospace Research and Development THERMO-MOLECULAR PRESSURE EFFECTS IN TUBES AND AT ORIFICES Max Kinslow and George D. Arney, Jr August 1967 57 pages incl. 22 refs, 25 figs.</p> <p>An investigation of the errors arising from thermal nonequilibrium in systems measuring gas pressures is presented. The errors are attributed to a phenomenon referred to as thermo-molecular pressure. This effect is investigated both theoretically and experimentally at sensing orifices and in tubes. A thorough review of the literature is given and a</p> <p style="text-align: right;">P. T. O.</p>	<p style="text-align: center;">532.522:532.575.6</p>	<p>AGARDograph 119 North Atlantic Treaty Organization, Advisory Group for Aerospace Research and Development THERMO-MOLECULAR PRESSURE EFFECTS IN TUBES AND AT ORIFICES Max Kinslow and George D. Arney, Jr August 1967 57 pages incl. 22 refs, 25 figs.</p> <p>An investigation of the errors arising from thermal nonequilibrium in systems measuring gas pressures is presented. The errors are attributed to a phenomenon referred to as thermo-molecular pressure. This effect is investigated both theoretically and experimentally at sensing orifices and in tubes. A thorough review of the literature is given and a</p> <p style="text-align: right;">P. T. O.</p>	<p style="text-align: center;">532.522:532.575.6</p>

theory is developed for the error introduced in the limiting case of a very small sensing orifice with heat flux to the orifice surface. The theory takes into account the effect of arbitrary thermal accommodation coefficient at the orifice surface. Experimental data are presented separately for thermo-molecular pressures in tubes and at orifices. In addition, results of heat-transfer measurements in the transitional flow regime between flat plates are presented as a basis for correlating the orifice data. Finally, methods are given, with examples, for the correction of thermo-molecular effects both at orifices and in circular tubes.

This is one of a series of publications by the NATO-AGARD Fluid Dynamics Panel. Professor Wilbur C. Nelson of The University of Michigan is the Editor

theory is developed for the error introduced in the limiting case of a very small sensing orifice with heat flux to the orifice surface. The theory takes into account the effect of arbitrary thermal accommodation coefficient at the orifice surface. Experimental data are presented separately for thermo-molecular pressures in tubes and at orifices. In addition, results of heat-transfer measurements in the transitional flow regime between flat plates are presented as a basis for correlating the orifice data. Finally, methods are given, with examples, for the correction of thermo-molecular effects both at orifices and in circular tubes.

This is one of a series of publications by the NATO-AGARD Fluid Dynamics Panel. Professor Wilbur C. Nelson of The University of Michigan is the Editor

theory is developed for the error introduced in the limiting case of a very small sensing orifice with heat flux to the orifice surface. The theory takes into account the effect of arbitrary thermal accommodation coefficient at the orifice surface. Experimental data are presented separately for thermo-molecular pressures in tubes and at orifices. In addition, results of heat-transfer measurements in the transitional flow regime between flat plates are presented as a basis for correlating the orifice data. Finally, methods are given, with examples, for the correction of thermo-molecular effects both at orifices and in circular tubes..

This is one of a series of publications by the NATO-AGARD Fluid Dynamics Panel. Professor Wilbur C. Nelson of The University of Michigan is the Editor

theory is developed for the error introduced in the limiting case of a very small sensing orifice with heat flux to the orifice surface. The theory takes into account the effect of arbitrary thermal accommodation coefficient at the orifice surface. Experimental data are presented separately for thermo-molecular pressures in tubes and at orifices. In addition, results of heat-transfer measurements in the transitional flow regime between flat plates are presented as a basis for correlating the orifice data. Finally, methods are given, with examples, for the correction of thermo-molecular effects both at orifices and in circular tubes.

This is one of a series of publications by the NATO-AGARD Fluid Dynamics Panel. Professor Wilbur C. Nelson of The University of Michigan is the Editor

